

RESEARCH ARTICLE

Open Access

# Histone H4 deacetylation plays a critical role in early gene silencing during neuronal apoptosis

Heather R Pelzel<sup>1,2</sup>, Cassandra L Schlamp<sup>2</sup> and Robert W Nickells<sup>\*2,3</sup>

## Abstract

**Background:** Silencing of normal gene expression occurs early in the apoptosis of neurons, well before the cell is committed to the death pathway, and has been extensively characterized in injured retinal ganglion cells. The causative mechanism of this widespread change in gene expression is unknown. We investigated whether an epigenetic change in active chromatin, specifically histone H4 deacetylation, was an underlying mechanism of gene silencing in apoptotic retinal ganglion cells (RGCs) following an acute injury to the optic nerve.

**Results:** Histone deacetylase 3 (HDAC3) translocates to the nuclei of dying cells shortly after lesion of the optic nerve and is associated with an increase in nuclear HDAC activity and widespread histone deacetylation. H4 in promoters of representative genes was rapidly and indiscriminately deacetylated, regardless of the gene examined. As apoptosis progressed, H4 of silenced genes remained deacetylated, while H4 of newly activated genes regained, or even increased, its acetylated state. Inhibition of retinal HDAC activity with trichostatin A (TSA) was able to both preserve the expression of a representative RGC-specific gene and attenuate cell loss in response to optic nerve damage.

**Conclusions:** These data indicate that histone deacetylation plays a central role in transcriptional dysregulation in dying RGCs. The data also suggests that HDAC3, in particular, may feature heavily in apoptotic gene silencing.

## Background

Intrinsic apoptosis in neurons culminates in BAX activation and translocation to the mitochondria, the release of cytochrome c, and the activation of the caspase cascade. BAX translocation marks the committed step of the cell death process [1]. Therefore, investigation of the apoptotic pathway prior to BAX involvement is an important element of developing strategies to intervene in neuronal cell death.

An early event in apoptosis is silencing of normal gene expression. In addition to this, new transcription, required for apoptosis, is activated. This change in transcriptional profile occurs in several models of neurodegeneration, including Huntington's Disease, Alzheimer's Disease, Parkinson's Disease, amyotrophic lateral sclerosis, spinocerebellar ataxia type 3, and the optic neuropathy glaucoma [2-10]. In glaucoma, retinal ganglion cells (RGCs) execute a typical intrinsic apoptotic program. Changes in transcription of several genes in injured

RGCs have been shown in experimental glaucoma and after acute injury to the optic nerve. Genes that decrease in expression in RGCs include several that are specifically expressed in these cells, such as *Thy1*, *Brn3b*, *Nrn1*, *Fem1c*, and *Sncg*, [3-5,11-16], as well as several non-cell type specific genes, including *BclX<sub>L</sub>*, *TrkB*, and members of the neurofilament gene family [3,13,14,17]. Of the genes with increased expression, the majority are proapoptotic or stress response genes, such as *Bim*, *cJun*, and several *Hsps* and caspases [4,5,18-20]. This change in the pattern of gene expression in RGCs occurs before detectable cell loss [4,11,21] and can also be induced by optic nerve crush (ONC) of *Bax* knock-out RGCs, indicating that this event occurs early in the apoptotic pathway. Little investigation has been conducted to understand the mechanism underlying the down-regulation of normal gene expression. The global nature of gene silencing in RGCs, however, suggests that epigenetic changes of the chromatin of actively transcribed genes may be an early step in apoptosis.

Post-translational modifications of histones are well known epigenetic changes that regulate chromatin folding, organization, and gene activity [22]. Histone modifi-

\* Correspondence: nickells@wisc.edu

<sup>2</sup> Department of Ophthalmology and Visual Science, University of Wisconsin, 3310 University Ave, Suite 206, Madison, WI, 53706, USA  
Full list of author information is available at the end of the article

cations include phosphorylation, methylation, ubiquitination, and/or acetylation of lysine residues principally in the N-terminal tails [23]. While all of these modifications have an effect on the transcriptional activity, acetylation has the most direct effect [24]. Acetylated histones are typically found in transcriptionally active euchromatic chromatin, whereas transcriptionally inactive heterochromatic chromatin is rich in deacetylated histones. Theoretically, deacetylation is thought to lead to a more compact chromatin structure, which limits access of transcription factors [24]. Alternatively, acetyl groups may facilitate the interactions of chromatin with specific transcription factors containing bromodomains, which recognize and bind acetylated amino acids of other proteins, including histone tails [25]. The acetylation and deacetylation of histones is controlled by opposing protein families called histone acetyltransferases (HATs) and histone deacetylases (HDACs).

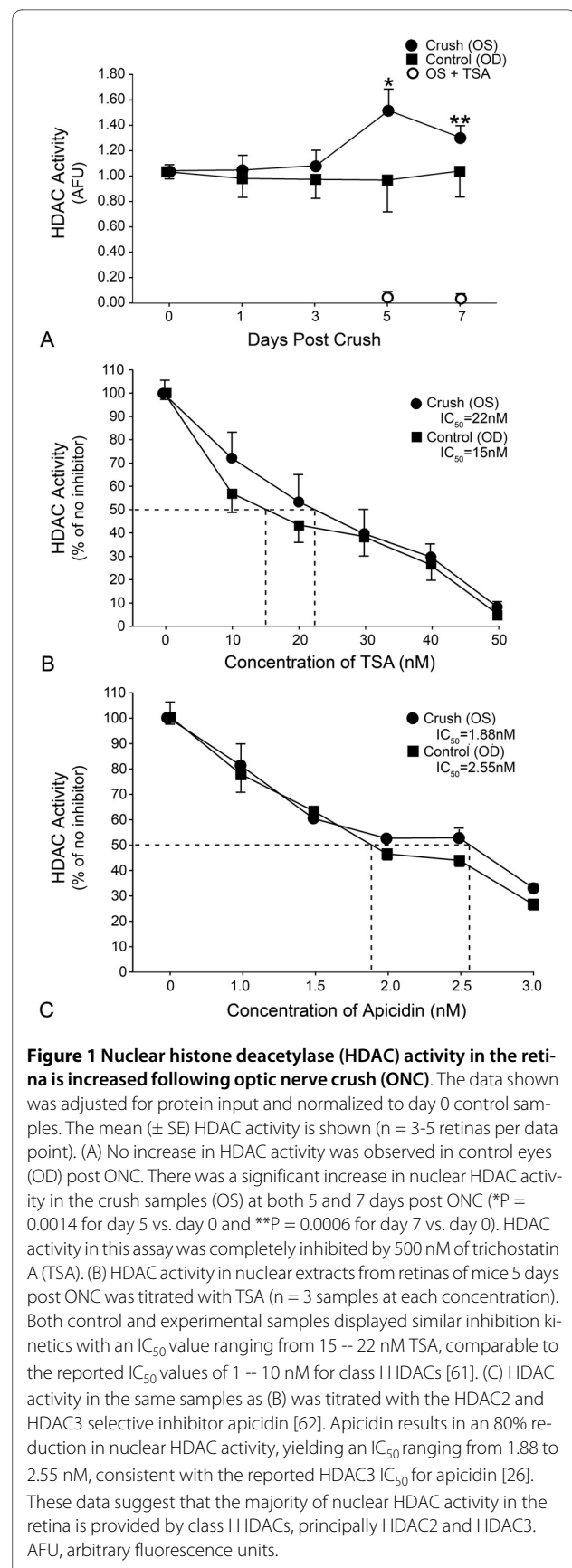
Here we show that several RGC specific genes, which decrease in expression after ONC, exhibit a decrease in promoter histone acetylation. This deacetylation is accompanied by an increase in both HDAC2 and HDAC3 expression and the translocation of HDAC3 to the nuclei of dying RGCs. Additionally, inhibition of HDAC activity is able to prevent the ONC-mediated silencing of at least one RGC-specific gene and attenuate the level of RGC death. These results represent one of the first documentations of epigenetic changes associated with neuronal cell death and may provide insight into some of the earliest changes occurring in dying RGCs.

## Results

### Nuclear HDAC activity is increased after ONC

Nuclear HDAC activity was measured in retinal nuclear protein extracts isolated at 1, 3, 5, and 7 days following ONC (Figure 1A). No significant change was detected in fellow control eyes (OD). Experimental eyes (OS) exhibited an ~50% increase in activity at day 5 post ONC ( $P = 0.0014$ ). Activity was also significantly higher than control eyes at 7 days post ONC ( $P = 0.0006$ ), although lower than day 5 experimental eyes. Nuclear HDAC activity in experimental and control eyes was completely inhibited by trichostatin A (TSA), indicating the presence of predominantly class I and II HDACs in this fraction (Figure 1A).

Dose-dependent inhibition of nuclear HDAC activity was also performed with different inhibitors to help evaluate which HDACs were active both before and after ONC. TSA-mediated inhibition of control and crush nuclear extracts from day 5 retinas showed a dose-dependent decrease in HDAC activity with an  $IC_{50}$  ranging from 15 to 22 nM (Figure 1B). A similar loss of activity was observed in extracts treated with the selective class I inhibitor, valproic acid (data not shown). To further refine



which class I HDACs may be contributing to the retinal nuclear activity, we repeated this experiment using apicidin, which is selective for HDACs 2 and 3. HDAC activity was also nearly completely inhibited with apicidin, yielding an  $IC_{50}$  ranging from 1.88 to 2.55 nM (Figure 1C). These values agreed with the reported  $IC_{50}$  value for HDAC3 (2.5 nM) using this inhibitor [26] and suggest that HDACs 2 and 3 contribute the majority of nuclear HDAC activity in the retina.

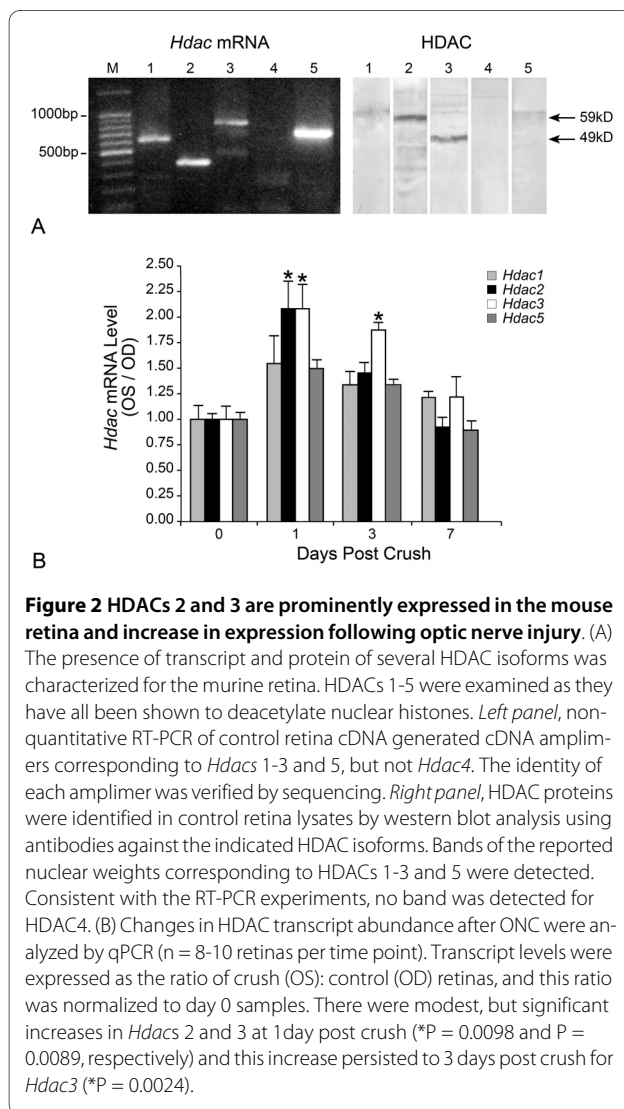
In addition to measuring nuclear HDAC activity, we also characterized which HDACs were expressed in the mouse retina by both mRNA and protein analysis. HDACs 1-5 were selectively examined because they have all been reported to be active in nuclei and are known to affect histone acetylation levels [27]. By RT-PCR and western blot analysis, HDACs 1, 2, 3, and 5, but not HDAC4 were detected in normal retinas (Figure 2A). At the protein level, bands of 59 kD and 49 kD, correspond-

ing to HDACs 2 and 3, respectively, appeared to be most abundant. This is similar to a previous report of the pattern of HDACs expressed in normal brain tissue [27]. To examine the change in HDAC expression in response to ONC, quantitative RT-PCR (qPCR) analysis was conducted on samples isolated from several time points following surgery (Figure 2B). By 1 day post ONC, the mRNAs for *Hdac*s 2 and 3 doubled ( $P = 0.0098$  and  $P = 0.0089$ , respectively), while transcripts for *Hdac*s 1 and 5 showed modest, but not significant increases. At 3 days post ONC, only *Hdac*3 transcripts remained significantly elevated ( $P = 0.0024$ ). By 7 days post ONC, no significant elevation of any of the examined *Hdac*s was detected.

### HDACs 2 and 3 in injured retinas

Since both *Hdac* 2 and 3 transcripts showed a significant increase following ONC and the majority of HDAC activity was sensitive to apicidin, we characterized these HDACs in the retina before and after ONC. To determine the localization of these isoforms, immunofluorescence was performed on retinal cryosections from control and crush eyes. Both HDAC2 and HDAC3 were present in cells of the ganglion cell layer (GCL) and inner nuclear layer (INL) of control eyes (Figure 3A). At higher magnification of the GCL of control retinas (Figure 3B, top panels), HDAC2 colocalized with 4,6-diamidino-2-phenylindole (DAPI), indicating that it was nuclear, consistent with reports that this is an exclusively nuclear protein [27]. In contrast, HDAC3 labeling was diffuse and appeared to be predominantly cytoplasmic with minimal overlap with DAPI labeling. This was also in agreement with previous reports that HDAC3 contains both a nuclear localization signal and a nuclear export signal [27], and can exist in both the cytoplasm and nuclei of cells [28].

Because subcellular localization of HDACs is a common mechanism of controlling HDAC activity [29], we also examined the distribution of HDAC2 and HDAC3 after ONC. In sections from retinas 3 days post ONC (Figure 3B, lower panels), HDAC2 remained localized to nuclei of the GCL. HDAC3 localization in the GCL, however, appeared to change after ONC, with cells showing both cytoplasmic and nuclear localization, as determined by colabeling with DAPI staining (Figure 3B and additional file 1: Localization of HDACs 2 and 3 before and after optic nerve crush). To confirm these findings, western blot analysis was conducted on nuclear and cytoplasmic fractions isolated from control and crush retinas. As shown in Figure 3C, a band at 59 kD, corresponding to HDAC2, was present in the nuclear fractions of both control and ONC retinas. A 49 kD band, corresponding to HDAC3, was present in the cytoplasmic fraction from control retinas, but was both cytoplasmic and nuclear in the experimental crush retinas consistent with the



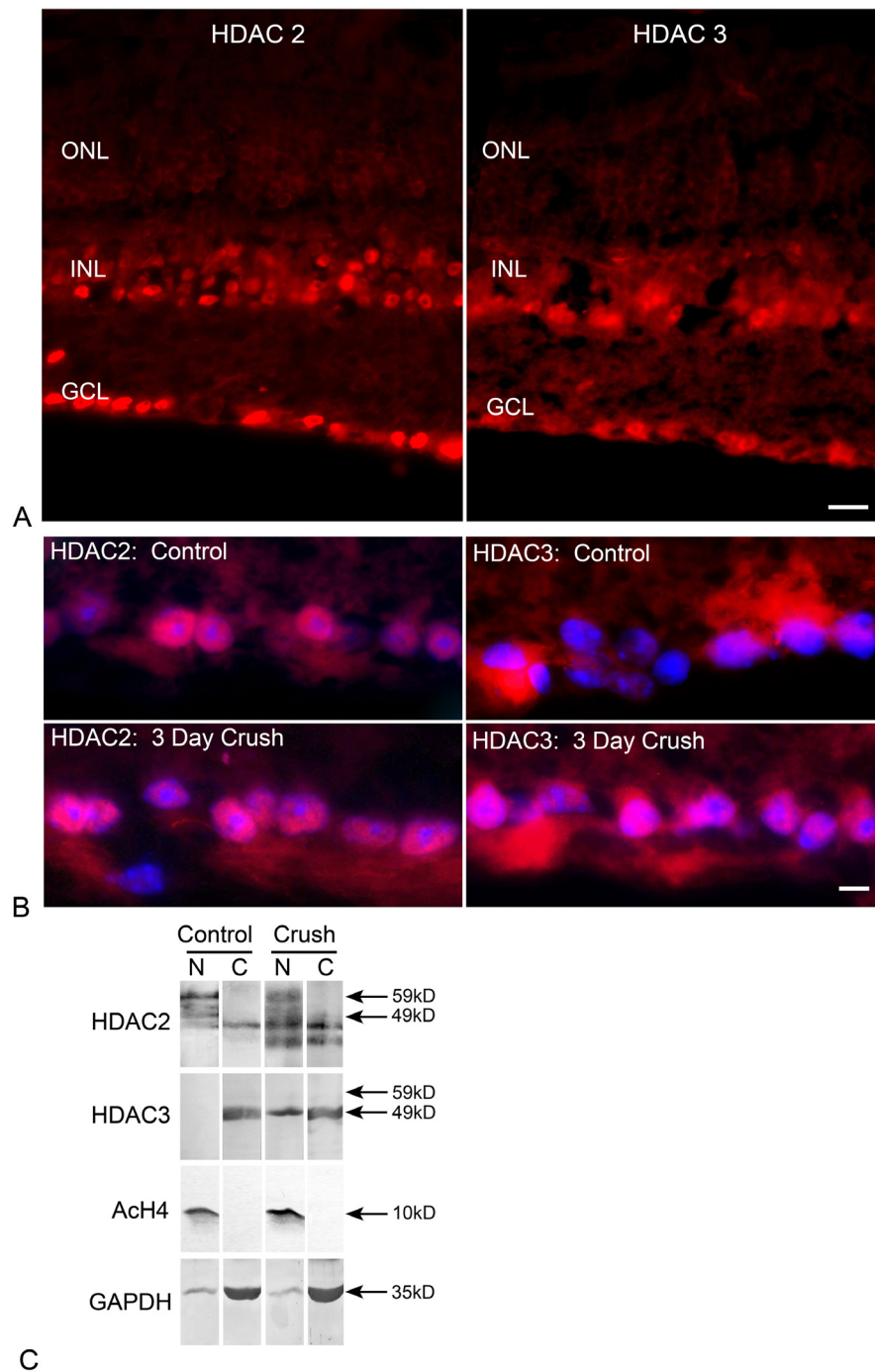


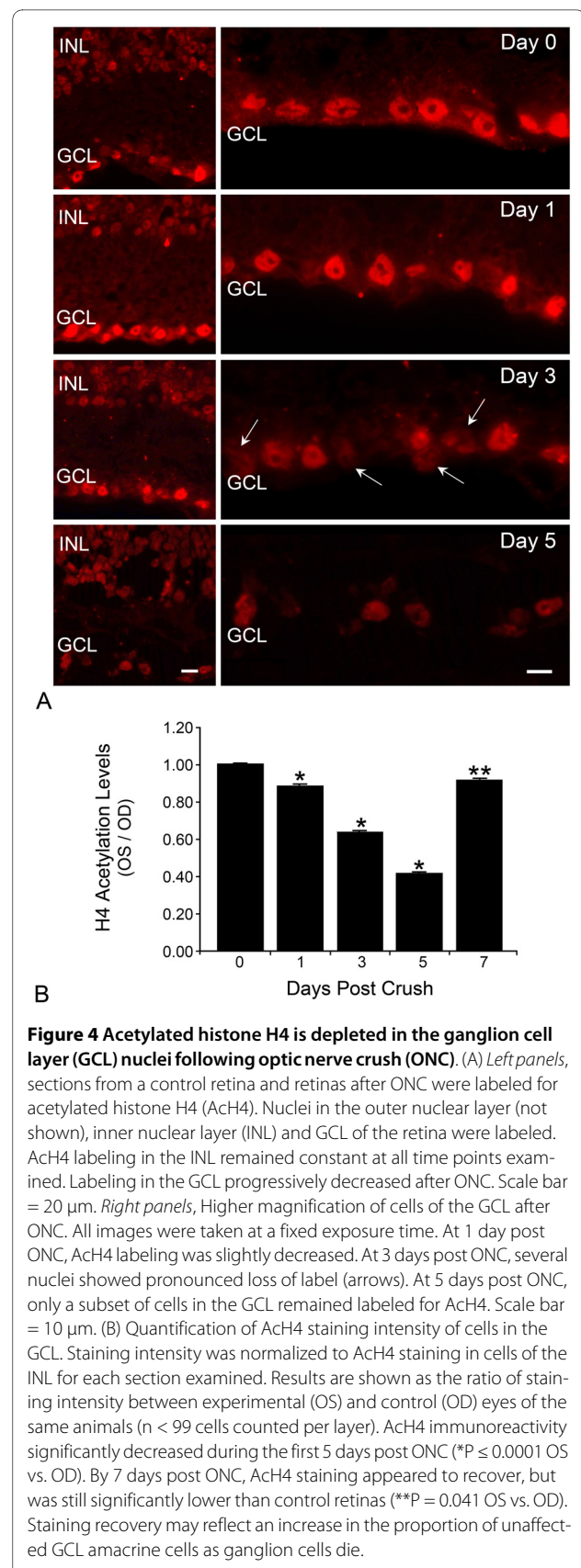
**Figure 3 HDAC2 and HDAC3 are expressed by cells in the ganglion cell layer (GCL).** (A) Nuclei in the GCL and inner nuclear layer (INL) were strongly labeled for HDAC2. HDAC3 labeling was more diffuse, but also labeled cells in the GCL and INL. Scale bar = 25  $\mu$ m. (B) Sections from control retinas and retinas 3 days after optic nerve crush. High-magnification images of the GCL are shown. Sections were counter-stained with DAPI to highlight nuclei. In control retinas, HDAC2 was localized to nuclei of GCL cells. HDAC3 labeling was principally in the cytoplasm of GCL cells, although some label appeared to be distributed in or around cellular nuclei. In the GCL of crush retinas, HDAC2 remained nuclear (lower left), while HDAC3 labeling was clearly detected in the nuclei of some cells. Scale bar = 5  $\mu$ m. Photomicrographs of the individual channels of these merged images are shown in additional file 1. (C) Western blot analysis of HDACs 2 and 3 in cytoplasmic (C) and nuclear (N) fractions of control and experimental retinas 3 days after optic nerve crush. A 59 kD band corresponding to HDAC2 was exclusive to the nuclear fractions in both control and crush retinas. The 49 kD band of HDAC3 was present only in the cytoplasmic fraction in the control eyes, but was distributed between both nuclear and cytoplasmic fractions in the crush samples suggesting nuclear translocation of HDAC3 after ONC. Control antibodies for Ach4 (nuclear) and GAPDH (cytoplasmic) are shown to monitor the relative purity of each fraction.

nuclear translocation of this protein after ONC. As a control for the fractionation, the blots were also probed for acetylated histone H4 and GAPDH as nuclear and cytoplasmic controls, respectively.

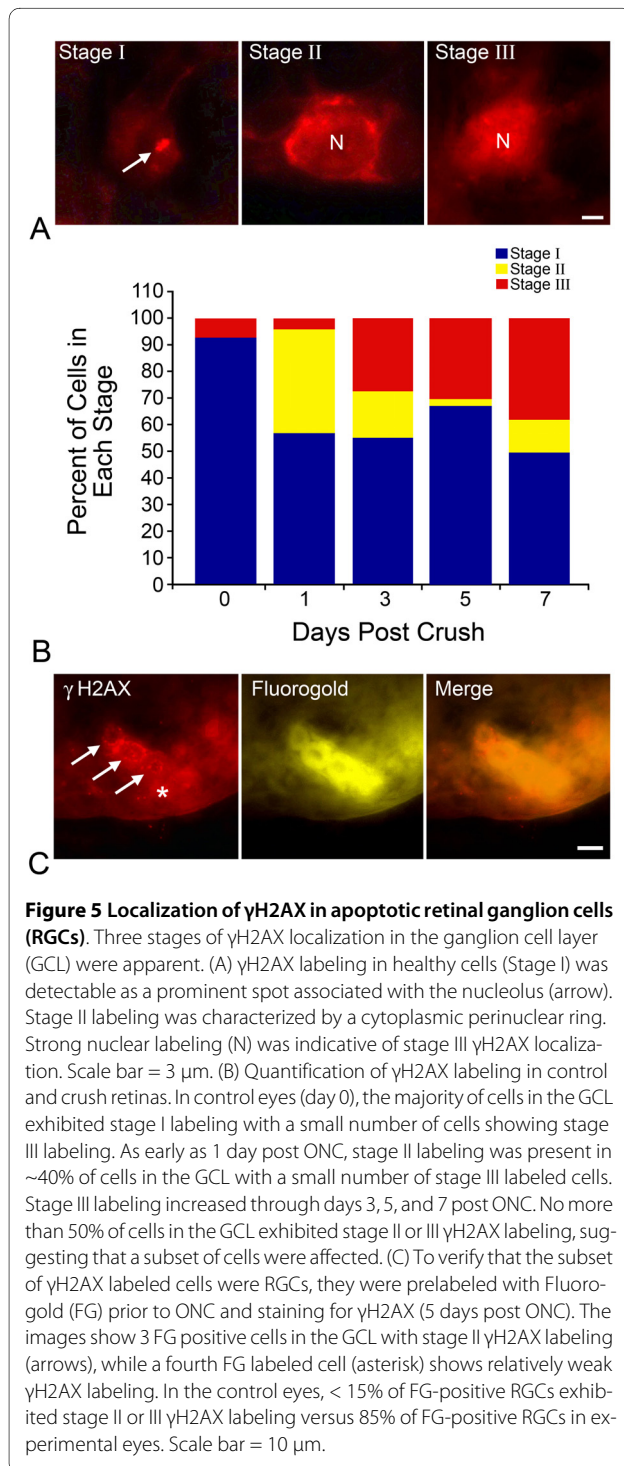
**Histone H4 acetylation in the GCL decreases following ONC**  
Histones H3 and H4 are substrates of HDACs 2 and 3. In particular, deacetylation of at least 5 different lysine residues of H4 have been implicated in transcriptional silencing [24]. To determine if there was a decrease in acetylation of histones in injured RGCs, concomitant with the increase in HDAC activity and increased nuclear presence, we examined retinal cryosections taken from control and experimental retinas with a polyclonal antibody against pan-acetylated histone H4 (ACh4). Figure 4A shows low magnification images of the INL and GCL (left panels), and higher magnification images of just the GCL (right panels). Nuclear labeling was detected in both the INL and GCL of the control retinas (top panels). After ONC, the label intensity remained consistent in the INL, but there was an apparent and progressive decrease in labeling of the GCL. High magnification images (Figure 4A, right panels) indicated that the decrease in label intensity was not only due to a loss of cells in this layer, but also to a decrease in the labeling of individual cells within this layer. To verify the decrease in label intensity of individual nuclei in the GCL, fluorescent pixel intensity of cells in this layer were measured and normalized to pixel intensity of ACh4 labeling in the INL of the same section. Compared to control eyes, the average ACh4 label intensity of GCL nuclei in experimental retinas progressively decreased to ~45% by 5 days post ONC (Figure 4B,  $P < 0.0001$  for days 1, 3, and 5 vs. control retinas). By 7 days post ONC, many RGCs are in the later stages of apoptosis [30]. Consistent with this, we observed an actual increase in the average ACh4 label intensity of cells remaining in this layer at 7 days. Although this average was still significantly below control levels ( $P = 0.04$ ), it may reflect that unaffected amacrine cells made up a larger proportion of nuclei assayed at this time point.

#### Characterization of HDAC3 translocation and deacetylation of histone H4 in dying cells

The increase in nuclear HDAC3 localization and an apparent decrease in histone H4 acetylation in some cells of the GCL following ONC is consistent with the concept of widespread histone deacetylation taking place in dying RGCs, which are the principal cell type affected by the crush procedure. Importantly, we wanted to verify that these changes were characteristic of dying cells. To address this, we first identified dying cells in retinal cryosections with an antibody against phosphorylated H2AX ( $\gamma$ H2AX). The phosphorylation of the histone H2A variant, H2AX, is a known marker of apoptosis, and its



appearance coincides with early onset DNA damage that precedes mitochondrial involvement in the cell death program [31]. In the GCL of injured retinas,  $\gamma$ H2AX underwent a progressive change in localization that allowed us to group the cells into three stages of  $\gamma$ H2AX labeling (Figure 5A). Stage I labeling was principally found in control retinas and in some GCL cells in injured



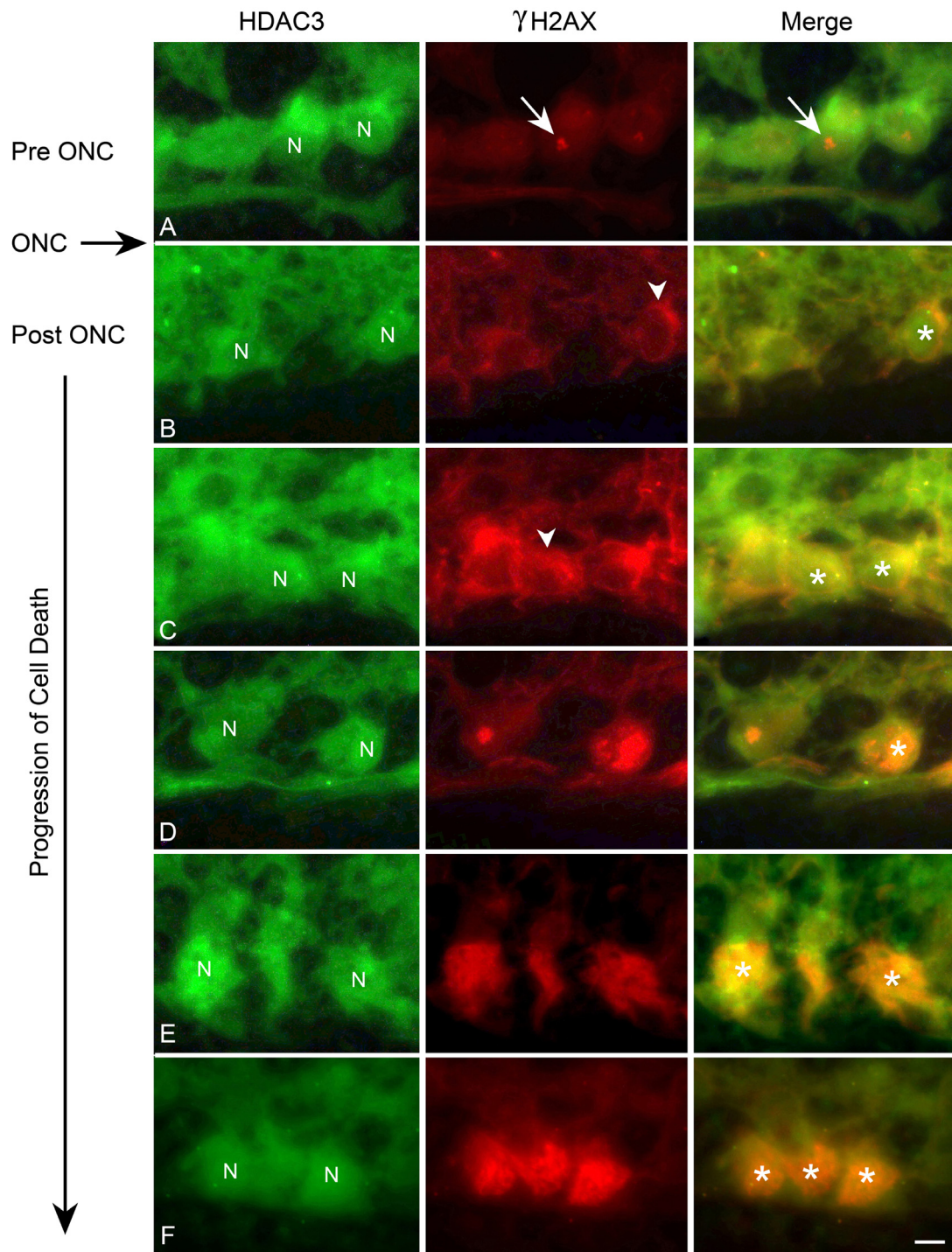
retinas and was characterized by little to no  $\gamma$ H2AX labeling except for a densely labeled spot associated with the nucleoli. Stage II was distinguishable by strong perinuclear labeling, while stage III had strong nuclear labeling. Stage II labeled cells began to appear in the injured GCL as early as 1 day post ONC. Progressively after this, an increasing proportion of cells exhibited stage III labeling. By 5-7 days post ONC, 50-60% of the cells in this layer were either stage II or stage III for  $\gamma$ H2AX, consistent with estimates that RGCs make up 60% of the cells in the GCL (Figure 5B) [32,33]. To verify labeling in RGCs, we also retrogradely labeled them with fluorogold prior to ONC. After crush surgery, an estimated 85% of the fluorogold positive cells exhibited stage II or stage III  $\gamma$ H2AX labeling (Figure 5C).

Figure 6 illustrates the change in HDAC3 and  $\gamma$ H2AX labeling in the retina as RGCs progressed through apoptosis. HDAC3 appeared to be cytoplasmic in control cells (Figure 6A), and shortly after ONC, was found co-localized with stage II  $\gamma$ H2AX labeled cells in the cytoplasm (Figure 6B). In other cells, however, HDAC3 staining was present in the nuclei, while  $\gamma$ H2AX staining was still localized as a perinuclear ring in the cytoplasm (Figure 6C). In mid-to late stages post ONC, double-labeled cells in the GCL exhibited stage III  $\gamma$ H2AX labeling and nuclear localization of HDAC3 (Figure 6D-F).

Because of the strictly nuclear presence of ACh4, the colocalization of ACh4 and  $\gamma$ H2AX was much different than that observed for HDAC3. In control eyes, the nuclei were strongly labeled for ACh4 and  $\gamma$ H2AX was only present as a spot that was associated with the nucleoli (Stage I, Figure 7A). Early after ONC, RGCs with stage II  $\gamma$ H2AX localization also presented with strong nuclear labeling with ACh4 (Figure 7B, C). In stage III labeled cells,  $\gamma$ H2AX and ACh4 colocalization was initially yellow in merged images, but progressed to orange, then red, indicative of both an increase in  $\gamma$ H2AX intensity and a decrease in ACh4 labeling (Figure 7D-F). The nuclear localization of this co-labeling was confirmed with DAPI staining, which also indicated that cells with nuclear  $\gamma$ H2AX and decreased ACh4 staining exhibited fragmented and condensed nuclei typical of apoptotic cells (See additional file 2: The deacetylation of histone H4 occurs in cells with nuclear  $\gamma$ H2AX and DNA fragmentation).

#### Promoter deacetylation is associated with a downregulation of gene expression in injured RGCs

To correlate the observed decrease in histone H4 acetylation with gene silencing, we determined if H4 deacetylation occurred in transcriptionally significant sites, such as the promoter regions of genes that are downregulated in RGCs in response to ONC. Following ONC, a number of genes are known to decrease in expression. A retrospec-



**Figure 6 HDAC3 translocates to the nuclei of apoptotic cells.** Retinal sections from eyes before optic nerve crush (ONC) and at several points after ONC were double labeled with antibodies against HDAC3 (green) and  $\gamma$ H2AX (red), to identify apoptotic cells (see Figure 5). (A) Cells in the ganglion cell layer prior to ONC exhibited diffuse cytoplasmic HDAC3 labeling and a densely labeled spot of  $\gamma$ H2AX (stage I labeling), which associated with the nucleoli (arrows). Representative unlabeled nuclei are indicated (N). (B) Following ONC, HDAC3 labeling began to appear in the nuclei (asterisk in merged image), while  $\gamma$ H2AX labeling was detectable as a cytoplasmic perinuclear ring (stage II labeling, arrowhead). (C) HDAC3 labeling continued to increase in the nuclei (asterisks), while the overall intensity of  $\gamma$ H2AX labeling increased in both the cytoplasm (arrowhead) and the nuclei, which appear yellow in the merged image (asterisks). (D) At later time points post ONC, a greater proportion of cells exhibited nuclear colocalization of HDAC3 and  $\gamma$ H2AX (stage III labeling, arrowhead). (E, F) HDAC3 and  $\gamma$ H2AX labeling continued to colocalize (asterisks), although nuclei of dying cells were less well defined. Scale bar = 5  $\mu$ m.

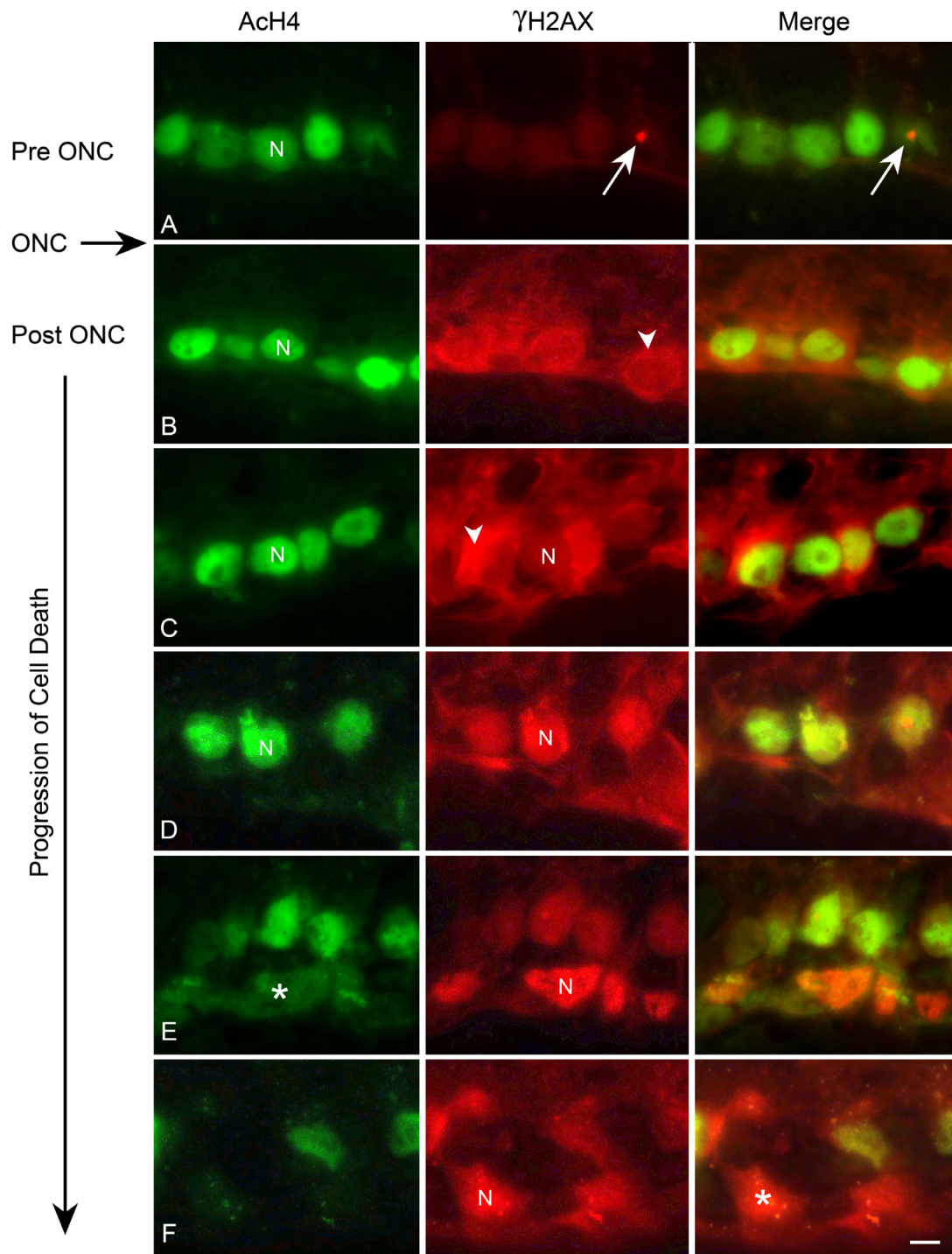


**Figure 7 Widespread deacetylation of histone H4 occurs in apoptotic cells.** Retinal sections from eyes before optic nerve crush (ONC) and at several points after ONC were double labeled with antibodies against acetylated histone H4 (AcH4, green) and  $\gamma$ H2AX (red), to identify apoptotic cells (see Figure 5). (A) Control ganglion cell layer nuclei (N) were strongly labeled for AcH4. Arrows indicate focal  $\gamma$ H2AX labeling associated with nucleoli (stage I). (B) Shortly after ONC,  $\gamma$ H2AX labeling became more apparent as a perinuclear ring, principally localized to the cytoplasm (arrowhead, stage II), while nuclei of these cells still exhibited strong labeling for AcH4. (C, D, E) At subsequent time points after ONC,  $\gamma$ H2AX labeling in nuclei (N) progressively increased (stage III), while nuclear AcH4 labeling decreased (asterisk in E). Note a change from green to yellow to red nuclear color in the merged panels. (F) By late in the cell death process, nuclei (N) intensely labeled for  $\gamma$ H2AX exhibited little to no immunoreactivity to AcH4 (asterisk). Scale bar = 5  $\mu$ m. The decrease in AcH4 labeling, and the presence of  $\gamma$ H2AX stage III labeling, also correspond to increased DNA fragmentation as assessed by DAPI staining (See additional file 2).



tive analysis of the literature indicated that the rapid decrease in transcript abundance for a majority of genes roughly follows an exponential decay curve (Figure 8A). To verify this in a controlled setting, we developed a mini qPCR array of several mRNAs expressed in RGCs and used it to monitor the change in transcript abundance in retinas over the first 7 days post ONC. Similar to the literature reports, this prospective study also showed the exponential decay of RGC transcripts (Figure 8B). Two sets of genes were examined for chromatin immunoprecipitation (ChIP) analysis. The first group included *Thy1*, *Brn3b*, *Nrn1*, and *Fem1c*, which are expressed predominantly by RGCs in the retina, as well as the anti-apoptotic gene *BclX* [3-5,11,14,15]. This group of genes represented a subset of genes that exhibit a reported decrease in expression after ONC. The second group of genes, *Bim* and *cJun*, were examined because they undergo an increase in expression following ONC [5,18]. ChIP assays, with antibodies against acetylated H4, were performed on retinas from control and crush eyes followed by qPCR to quantify the genomic DNA that was collected. The quan-

tification of promoter DNA associated with acetylated histone H4 is shown in Figure 9 and is expressed as a ratio of experimental: control retinas. All ratios have been normalized to day 0 controls. Surprisingly, promoter regions for both down-regulated and up-regulated genes showed a significant decrease in histone acetylation 1 day post ONC, with the exception of the promoter for *cJun* (Figure 9A). Three days post ONC, however, the acetylation pattern of promoter histones was changed and only down-regulated genes exhibited a decrease in promoter acetylation (Figure 9B), while promoter H4 acetylation for *cJun* had remained at day 0 levels and levels for *Bim* had significantly increased ~2-fold. A similar pattern of promoter acetylation observed 3 days after ONC was also evident on day 5 post ONC (Figure 9C), except that *Bim* H4 promoter acetylation had increased further to ~3-fold the level detected in day 0 retinas.

#### Inhibition of HDAC activity blocks ONC-induced silencing of the *Fem1c*<sup>R3</sup> reporter gene

Although promoter histone deacetylation is associated with silenced genes in RGCs, these experiments do not

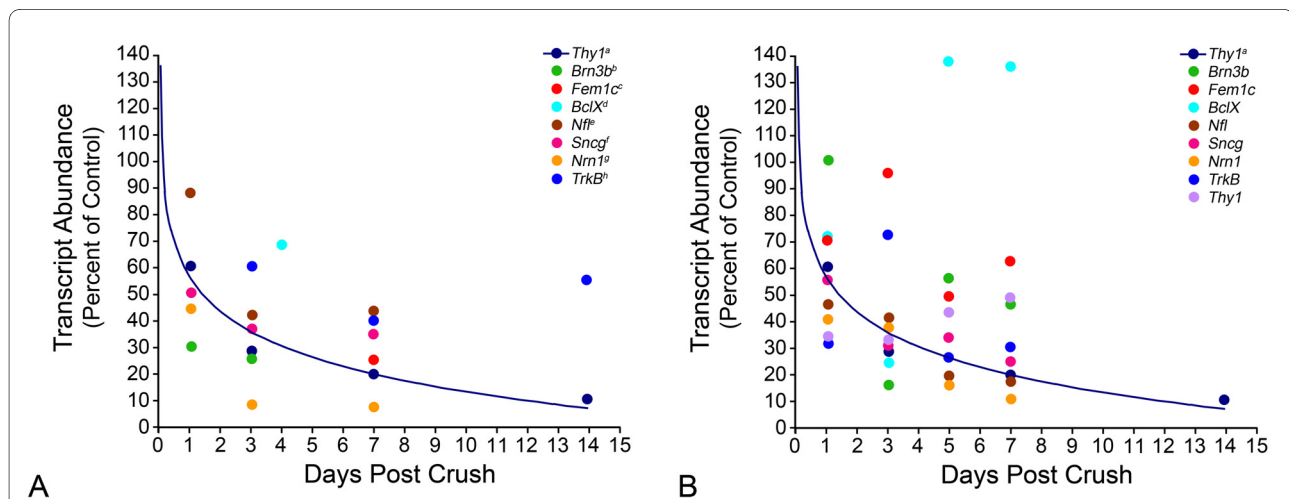


**Figure 8 Progressive gene silencing following optic nerve crush (ONC) precedes the loss of retinal ganglion cells (RGCs).** Analysis of transcript levels of several silenced genes following ONC or optic nerve axotomy. (A) A retrospective analysis of published reports of gene silencing in apoptotic RGCs. Each data point represents the mean of values collected by different investigators to simplify the data set shown. One of the earliest demonstrations of gene silencing in RGCs after optic nerve damage was a quantitative RNase protection assay study for the RGC marker gene *Thy1* [11]. These data points follow an exponential decay curve described by the equation,  $y = -18.441 \ln(x) + 55.703$ . All other data points are shown relative to this curve and displayed similar kinetics of silencing. Alternatively, during the first 7 days after ONC less than 1% of the cells had been eliminated (data not shown) [11]. Thus, gene silencing precedes cell loss by several days and represents a relatively early event in the apoptotic pathway. (B) Quantitative PCR analysis of silenced genes following ONC, graphed over the exponential decay curve of the original *Thy1* study. A similar decline in transcripts is evident in a more controlled prospective study. Interestingly, after an initial decline, *BclX* levels recover, consistent with earlier reports. In addition, genes with increases or no change in expression were also examined. Both *Gap43* and *Bim* exhibited increases in transcript level in the experimental eye following ONC (145% and 116%, respectively), while *S16* remained unchanged (99.8%, data not shown). In independent qPCR experiments, *cJun* transcript levels were also observed to increase modestly, shortly after ONC (112%).

<sup>a</sup>[11] Transcript abundance quantified by RNase protection assays in mouse ONC.  
<sup>b</sup>[15] Quantified by qPCR in a rat model of axotomy.  
<sup>c</sup>[12] Protein levels quantified by ELISA assays in mouse ONC.  
<sup>d</sup>[14] Transcript abundance quantified by RNase protection assay in rat ONC.  
<sup>e, f, g</sup>[5] Quantified by qPCR following axotomy in rats.  
<sup>h</sup>[17] Transcript abundance measured by quantitative in situ hybridization studies following axotomy in rats.

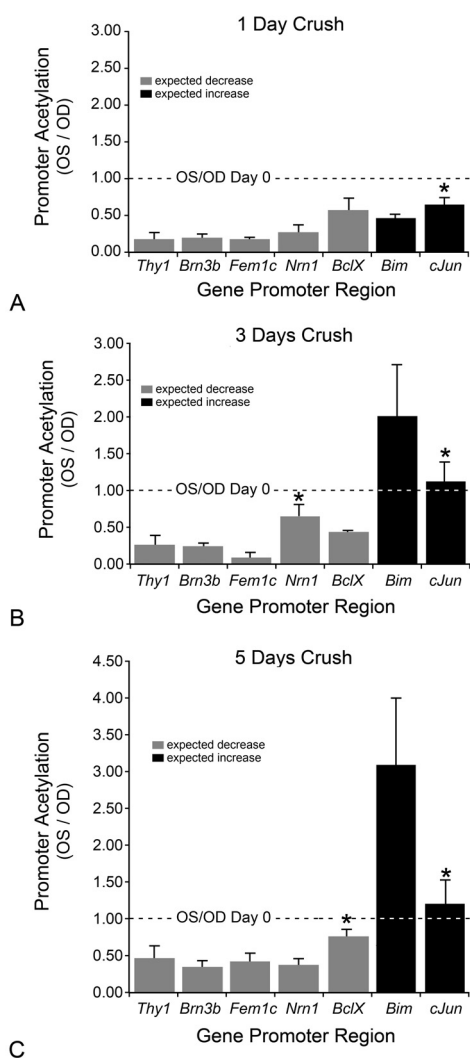


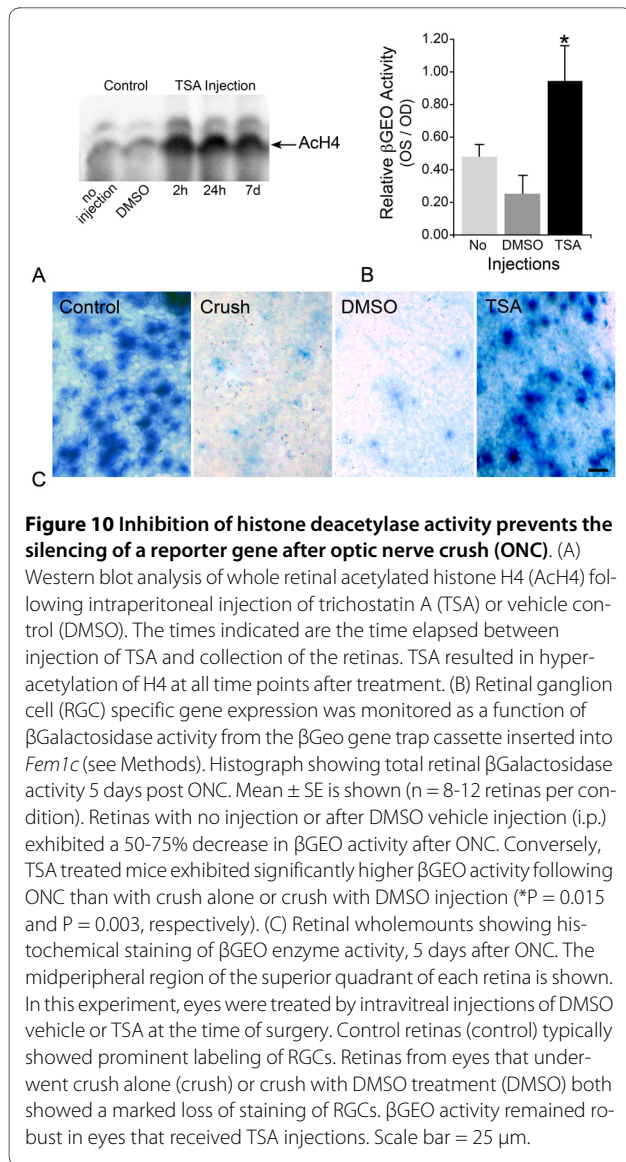
**Figure 9 Gene promoter associated histone H4 becomes deacetylated following optic nerve crush (ONC).** Two gene sets were examined by chromatin immunoprecipitation for acetylated H4. The first was comprised of genes whose expression had been documented to decrease during ganglion cell apoptosis (grey bars), including *Thy1*, *Brn3b*, *Fem1c*, *Nrn1*, and *BclX* (see text). The second set consisted of a pair of genes (*Bim* and *cJun*) whose expression has been documented to increase during apoptosis (black bars). The data is shown as a ratio of crush (OS)/control (OD) and has been normalized to day 0 levels (dashed line) (n = 6 samples at each time point). (A) At 1 day post ONC, there was a significant decrease in promoter H4 acetylation of most of the genes examined (range of P values was  $9.9 \times 10^{-5}$  for *Thy1* to 0.04 for *Bim*). Promoter acetylation for *cJun* was decreased, but this was not significant compared to day 0 levels (\*P = 0.08). (B) At 3 days post ONC, the decrease in promoter acetylation persisted for down-regulated genes. Conversely, the promoters of genes that are typically up-regulated exhibited a detectable increase in H4 acetylation to normal or above-normal levels. All changes were significantly different compared to day 0 levels, with the exceptions of *Nrn1* and *cJun* (\*P > 0.08). (C) The general pattern of H4 acetylation observed at 3 days post ONC, remained consistent through 5 days post ONC. Promoters for *BclX* and *cJun* exhibited no statistical change from day 0 histone acetylation levels at this stage (\*P > 0.1).

conclusively demonstrate that this epigenetic change is the controlling mechanism for transcriptional downregulation. To address this, we examined if inhibitors of HDAC activity could block the ONC-mediated downregulation of RGC-specific gene expression. For these experiments, we used *Fem1c*<sup>Rosa3</sup> (R3) mice, which contain the  $\beta$ Geo promoter trap reporter in the first intron of the *Fem1c* gene. Previously, we showed that mice express  $\beta$ GEO in an RGC-specific manner [12]. Additionally, we have observed a 75% decrease in  $\beta$ GEO total protein and enzyme activity [12], and a 50% decrease in *Fem1c* transcript levels, by 5 days post ONC (Figure 8A, B). Thus, the R3 reporter allows for the rapid detection and quantification of changes in RGC gene expression.

HDAC activity in the retina was inhibited by pretreatment of mice with TSA given as a single intraperitoneal (i.p.) injection, 24 hours before ONC. Western blot analysis of ACh4 levels in extracts of total retinal protein (Figure 10A) confirmed inhibition of HDAC activity, which was exemplified by hyperacetylation of H4. The effects of TSA were detected as quickly as 2 hours after injection and persisted as long as 7 days post injection. R3 gene expression was assessed by  $\beta$ GEO solution assays 5 days post ONC (Figure 10B). ONC resulted in a 55-75% decrease in  $\beta$ GEO enzyme activity by 5 days after surgery. TSA treated mice, however, exhibited significantly more activity at this time point than mice receiving no injection or DMSO injections (P = 0.016 and P = 0.003, respectively). In a separate series of experiments, TSA was also administered as a single intravitreal injection at the time of ONC surgery. Whole-mounted retinas from these experiments exhibited  $\beta$ GEO staining in RGCs consistent with the solution assays (Figure 10C). Taken together, these data suggested that TSA was able to attenuate the silencing of the *Fem1c* gene.

#### Inhibition of HDAC activity attenuates cell loss following ONC

Although histone deacetylation plays a role in modulating gene silencing during apoptosis, it is unknown if this process is a critical stage in the progression of the cell death program. To address this, we injected mice (i.p.) with the HDAC inhibitor, TSA, 24 hours prior to ONC. Retinas were then examined 2 weeks after surgery, which represents a point when there is normally significant cell loss [33]. The mice that underwent crush alone, or mice that received an injection of DMSO prior to ONC, exhibited comparable losses of  $36.4 \pm 3.4\%$  and  $31.2 \pm 2.9\%$  of cells in the GCL (P = 0.13, Figure 11A). Conversely, mice that received TSA prior to ONC showed a significant attenuation of cell loss in the GCL ( $14.4 \pm 5.3\%$ ) as compared to both crush alone and crush with DMSO (P = 0.005 and P = 0.01, respectively). Representative Nissl-stained whole mounts of retinas from a control eye and each of the

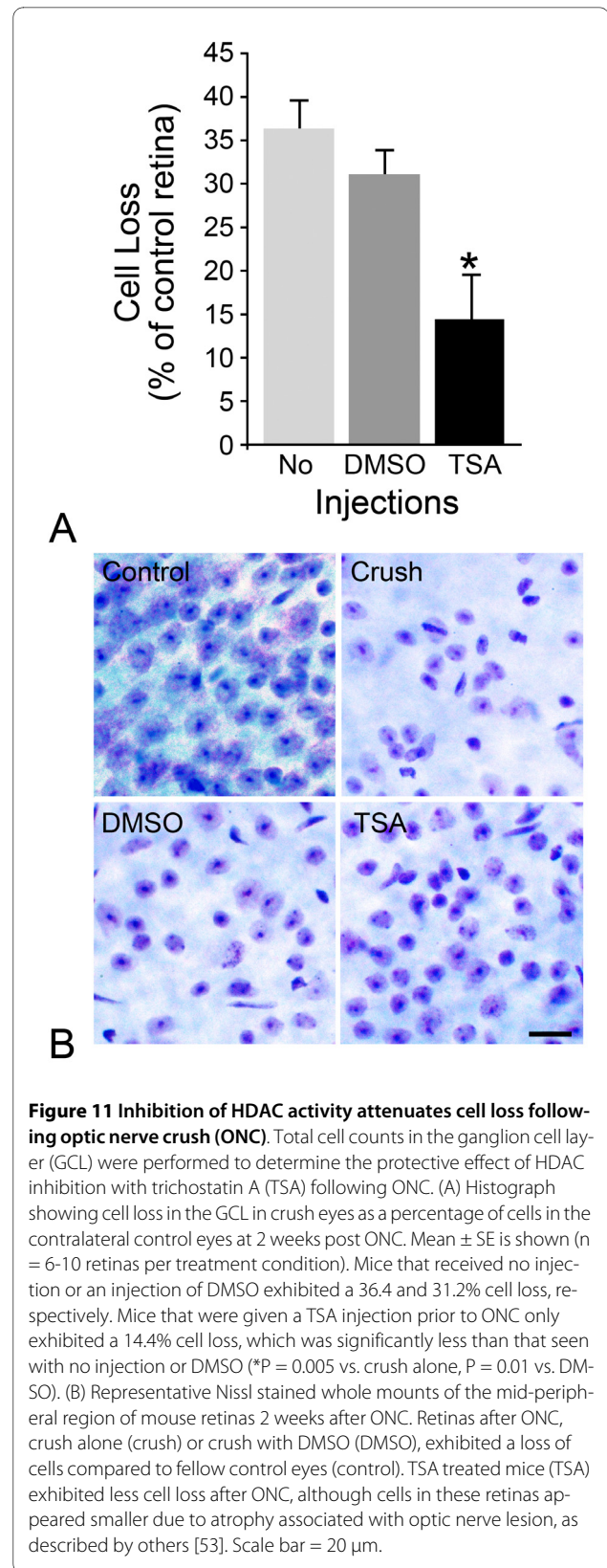


three treatments are shown in Figure 11B. Although cell loss was attenuated by treatment with TSA, surviving cells did exhibit signs of atrophy such as somal shrinkage.

## Discussion

Previous studies by our group and others have shown that silencing of normal gene expression is an early event in the apoptotic pathway of neurons, including RGCs [5,11,12,15]. Although microarray studies have carefully documented early gene expression changes in dying neurons, little attention has been given to understanding the causative mechanism leading to these widespread changes. Here we propose that epigenetic changes in active chromatin, specifically histone deacetylation, are part of the underlying mechanisms of apoptotic gene silencing.

We were able to detect an increase in whole retinal nuclear HDAC activity at the earliest time point exam-



ined (1 day post ONC), however, it was not significantly higher until day 5. This lag in HDAC activity may reflect that the increase was mainly occurring in the RGCs,

which only comprise 1-2% of the cell population in the retina. Therefore, day 5 post ONC may represent a point when a maximum number of RGCs were exhibiting an increase in HDAC activity. Conversely, because this experiment was performed on whole retina extracts and not on RGC-enriched samples, the increase in activity could possibly be due to changes in other cell types within the retina. The immunofluorescent studies examining changes in nuclear histone H4 acetylation, however, suggest that the changes in HDAC activity are likely limited to dying cells in the GCL.

Our experiments suggest that HDACs 2 and 3 play a central role in the process of histone deacetylation during RGC death. We have focused on HDAC3, principally because there is a sustained increase in transcripts for this gene after ONC, and HDAC3 protein translocates to nuclei of dying cells. It is reasonable to speculate that the movement of HDAC3 is a principal mechanism that increases nuclear HDAC activity in RGCs, and that this leads to the deacetylation of histone H4. We can infer the sequence of events defining the relationship between HDAC3 and the deacetylation of H4 by using the expression and localization of  $\gamma$ H2AX to identify the stage of the apoptotic pathway that any given cell is in (Figure 12 and additional file 3: The change in expression and cellular distribution of  $\gamma$ H2AX provides a temporal indicator of histone deacetylation in damaged ganglion cells). Early in dying cells (stage II  $\gamma$ H2AX), cytoplasmic HDAC3 appears to translocate to the nucleus in advance of  $\gamma$ H2AX nuclear localization. This is evident by cells, which exhibit stage II labeling but may be either cytoplasmic or nuclear for HDAC3. The majority of these cells are present by day 1 post ONC, and already show a quantifiable decrease in Ach4 (Figure 4). Additionally, qPCR data show significant increases in *Hdac 2* and *3* transcripts by this day, and ChIP analysis shows significant deacetylation of target promoters coincident with a dramatic decrease in transcript abundance from these target genes (Figures 8 and 9). Thus, by all accounts, a localized increase in nuclear HDAC activity that leads to gene silencing by promoter histone deacetylation appears to be a very early event in the response of the RGC soma after ONC.

The question that remains, however, is why does there appear to be a progressive increase in the level of nuclear HDAC activity and a similar progressive decrease in histone deacetylation after this initial silencing event? Part of the answer to this may lie in the relative sensitivity of the different assays used to detect changes in transcript abundance, promoter acetylation, HDAC activity, and H4 acetylation levels, but more likely the consequences of deacetylation are two-fold. The early onset of deacetylation may selectively target actively expressed genes, leading to gene silencing. Later, progressive and global

deacetylation may be required as the cell continues through the apoptotic pathway, in order to facilitate the condensation of the nuclear chromatin into a heterochromatic state. Chromatin condensation is one of the morphological hallmarks of apoptosis, and has been clearly documented in apoptotic RGCs [34,35]. Histone tails in condensed heterochromatin are generally hypermethylated and hypoacetylated [22]. HDAC3, in particular, may play a key role in chromatin condensation. Previous studies have shown that deacetylation of histone H3 by HDAC3 initiates chromatin condensation during mitosis by creating a preferred binding site for Aurora B kinase, which then phosphorylates H3 [36]. This modification of the histone code is the first of several events that eventually lead to chromatin condensation.

Although our experiments show that deacetylation of histones may be a central mechanism of transcriptional silencing, consistent with other reports [37,38], they do not exclude involvement of other chromatin modifications such as the methylation and demethylation of histones. Unlike the association between acetylation status of histones and transcriptional activity, the role of methylation in regulating transcription is more complicated. Trimethylation of lysine 4 in histone H3 (H3K4me3), for example, is associated with transcriptional activity, while trimethylation of H4K20 is associated with silent chromatin [24,39]. Additionally, HDAC activity is often closely linked to the activity of demethylases, since these enzymes are part of larger protein complexes. In both humans and mice, HDAC2 is often part of the REST complex, which also includes the histone demethylases RBP2 and AOF2 [40]. Similarly, HDAC3 is a component of the SMRT/N-CoR complex, which is able to associate with the histone demethylase JMJD2A [41]. Preliminary RT-PCR results from our laboratory have shown that transcripts for both *Ncor1* and *Ncor2* (the mouse homologs to *SMRT* and *N-COR*), as well as *Rcor2* (*COR-EST*) and *Aof2*, are present in the mouse retina (data not shown), indicating that the components for active HDAC3 and HDAC2 complexes are expressed in this tissue.

#### **Modulation of the HAT and HDAC activity balance during neurodegeneration**

In healthy cells, HAT and HDAC activities are balanced to regulate transcriptional activity [24]. The disruption of this balance, as demonstrated through the use of HDAC inhibitors, can lead to apoptosis principally in rapidly dividing cells [42,43]. Disruption of the HAT:HDAC balance also appears to play a role in neurodegenerative diseases, albeit by a mechanism that appears to be different from the lethal imbalances that cause cancer cell death. Rather than decreases, relative increases in HDAC activity contribute to the progression of neuronal apoptosis in

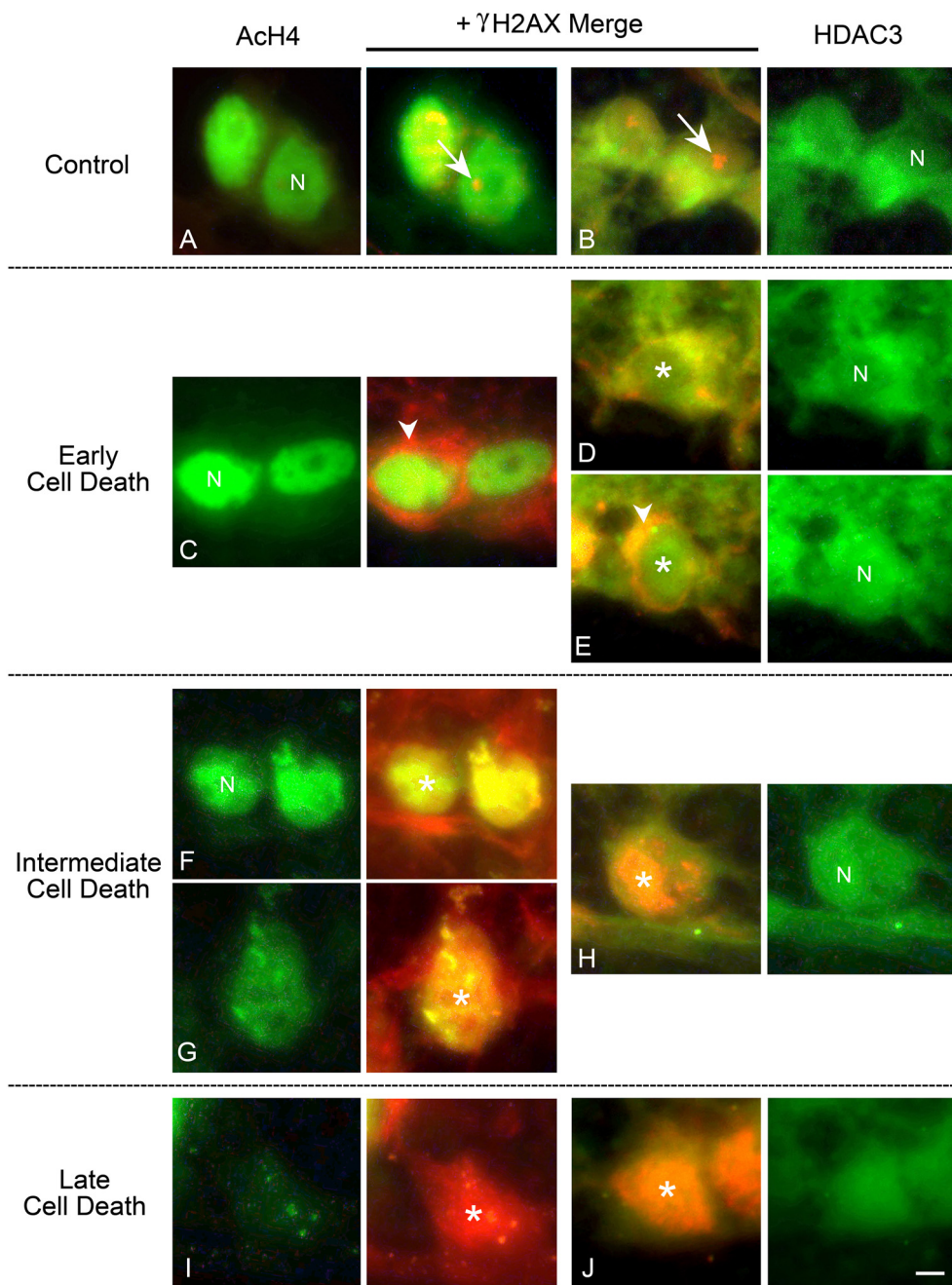


**Figure 12 HDAC3 becomes localized to nuclei prior to the deacetylation of histone H4 in dying cells.** Retinal cryosections before and after optic nerve crush (ONC) were colabeled with either  $\gamma$ H2AX and AcH4 or HDAC3 antibodies. Representative cells from the ganglion cell layer (GCL) are shown for four stages of  $\gamma$ H2AX localization. (A, B) Control retinas showed nuclear labeling of acetylated H4 (AcH4) and cytoplasmic labeling of HDAC3. Representative nuclei are indicated (N).  $\gamma$ H2AX was present as a densely labeled spot associating with the nucleoli (stage I labeling, Figure 5). (C) Early in the cell death process, nuclei (N) in the GCL were still brightly labeled for AcH4. At this stage,  $\gamma$ H2AX had begun to appear as a perinuclear ring (arrowhead) (stage II labeling) and was not colocalized with the nuclear AcH4. Conversely,  $\gamma$ H2AX did colocalize with HDAC3 at this stage. (D, E) These images illustrate the progressive movement of HDAC3 into the nuclei of dying cells. (D) HDAC3 was mainly present in the cytoplasm, but appeared to be concentrating around the nucleus (N). In E, HDAC3 was distributed in both the nucleus (asterisk in merged image), and colocalized with perinuclear  $\gamma$ H2AX (arrowhead). (F, G) After HDAC3 had begun to accumulate in the nuclei, a progressive decrease in AcH4 labeling was detected. Also at this point,  $\gamma$ H2AX was present in the affected nuclei (stage III labeling, asterisk in G). (H) HDAC3 labeling continued to increase in the nuclei and was now colocalized with nuclear  $\gamma$ H2AX (asterisk). (I, J) At this late stage of cell death, there was virtually no AcH4 left in the  $\gamma$ H2AX-labeled cells (asterisk in I), while  $\gamma$ H2AX and HDAC3 remained colocalized in the nuclei (asterisk in J). A graphic representation of these changes is also shown in additional file 2. Scale bar = 2  $\mu$ m.

several disease models [37,44,45]. One of the consequences of this imbalance could be an overall decrease in histone acetylation, which leads to a decrease in gene expression. Studies in which HDAC activity is suppressed by HDAC inhibitors, presumably restoring the HAT:HDAC balance, show that this treatment is able to attenuate neuronal apoptosis. Several groups investigating models of polyglutamine expansion neurodegenerative diseases, such as Huntington's disease, for example, have used HDAC inhibitors to prevent cell loss [38,46-48]. In these models, the relative increase in HDAC activity has been hypothetically attributed to a decrease in HAT activity resulting from the sequestration and degradation of the acetyltransferase, CREB binding protein (CBP) [38,46], while HDAC activity levels remain unchanged [49]. This model of neurodegeneration implies that the relative increase in HDAC activity is a passive consequence of the selective loss of CBP. Our data, although consistent with the idea that HDAC activity is relatively increased, suggest that this change is reflective of an active increase in nuclear HDAC levels in dying RGCs, associated with both a modest increase in HDAC gene expression and the translocation of an active protein. In fact, nuclear HAT activity assays show no significant changes in overall acetyltransferase activity in retinas harvested from eyes after ONC (data not shown).

The overall importance of HDAC activity in the process of RGC death can be probed with HDAC inhibitors such as TSA. TSA pretreatment was able to attenuate the down regulation of at least one gene normally expressed in RGCs (*Fem1c*<sup>R3</sup>). Consistent with the other reports showing a protective effect in models of neurodegeneration, TSA was also able to provide a modest protective effect to RGCs after ONC. The underlying cause for this latter effect is not known and may be due to a variety of factors, such as stabilizing the balance between HAT and HDAC activity or allowing for increased acetylation of factors such as Sp1, which has been shown to be neuroprotective in a model of hypoxic stress [50]. Conversely, it is equally possible that maintaining normal gene expression may have a secondary protective effect to the RGCs. For example, previously we showed that the anti-apoptotic gene *BclX* was down-regulated after optic nerve crush in rats [14]. Preventing this decrease could result in an increase in RGC resistance to a damaging stimulus by antagonizing the actions of proteins like BAX.

Although several studies have linked an increase in HDAC activity to neuronal death, others have demonstrated that the overexpression of HDACs can be neuroprotective. Chen and Cepko showed that the overexpression of HDAC4 led to increased protein stability of the transcriptional activator HIF1 $\alpha$ , which had a protective effect in a model of photoreceptor degeneration [51]. A related study demonstrated that part of the

beneficial effect of HDAC4 on HIF1 $\alpha$  transcriptional activity was due to HIF1 $\alpha$ 's increased ability to bind the histone acetyltransferase, p300 [52], which could be beneficial during neurodegeneration when fewer active HATs are available [37,44]. In these cases, the protective effect of increased HDAC activity appeared to be restricted to cytoplasmic activity on non-histone substrates.

Irrespective of the principal function of HDAC activity during cell death, the phenomenon of gene silencing is likely going to act as a barrier to regaining normal cell function in neuroprotective strategies. *Bax*-deficient RGCs, which are completely resistant to apoptosis after ONC, for example, can remain in a genetically silent, heterochromatic state for months following injury (unpublished data). Similarly, inhibition of HDAC activity using TSA, still resulted in some cell atrophy characterized by soma shrinkage. Shrinkage of RGCs after optic nerve damage has been described by others [53], including in *Bax*<sup>-/-</sup> RGCs [54]. This atrophy response may be indicative of the apoptotic volume decrease described in some neuronal cell types [55], which is considered to be a very early event in the apoptotic program and is regulated by a rapid efflux of intracellular potassium in many neurons, including retinal ganglion cells [56,57]. The effects we observe in TSA-treated mice suggest that epigenetic changes leading to gene silencing is downstream of the apoptotic volume decrease. Nevertheless, a complete understanding of the early changes in affected ganglion cells remains an important consideration for neuroprotective strategies. Clearly, regaining normal cell function will ultimately require reactivation of normal gene expression, meaning reversal of epigenetic changes associated with silenced genes.

## Conclusions

In summary, this study demonstrates that a change in histone acetylation levels, particularly in the promoter regions of silenced genes, may be part of the underlying mechanism of apoptotic gene silencing. In addition, there is some evidence indicating that HDAC3 may be the predominant HDAC isoform responsible for apoptotic histone deacetylation in dying RGCs. Initial HDAC inhibition studies indicate that TSA can prevent gene silencing and has a neuroprotective effect, suggesting that histone deacetylation may be a critical stage in the apoptotic pathway.

## Methods

### Experimental animals and optic nerve crush

All mice were handled in accordance with the Association for Research in Vision and Ophthalmology statement for the use of animals for research. The majority of experiments were conducted on CB6F1 mice, which have been used in the past by our group to quantify cell loss and

changes in RGC transcript levels, as a result of ONC. In some experiments, however, ROSA3, a substrain of C57BL/6 mice [12], were used to utilize the expression of  $\beta$ GEO marker protein as a way to more precisely quantify RGC-specific gene expression. These latter mice express  $\beta$ GEO as the result of transcription of the *Fem1c* gene, which is predominantly RGC-specific in the retina. They also exhibit similar kinetics of cell loss observed in the CB6F1 strain. For both strains, a random mixture of males and females between the ages of 4-6 months were used. ONC was performed unilaterally as described previously to initiate degeneration of the retinal ganglion cells [30]. Retinas were harvested 1, 3, 5, 7, or 14 days post ONC as indicated.

In some cases, retinal ganglion cells were retrogradely labeled with the tracer dye, fluorogold (Molecular Probes, Eugene, OR). Labeling was performed by first exposing the superior collicli on each side of the brain and placing a small piece of gel-foam, soaked in 0.9% NaCl containing 2% fluorogold, to each exposed surface. ONC surgery was performed 3 days after dye application.

#### HDAC activity assay and nuclear protein extraction

Nuclear proteins were extracted from whole retinas according to Andrews and Faller (1991). Protein concentration was determined using a BCA protein assay kit (Pierce, Rockford, IL). HDAC activity assays were performed using a Fluor de Lys kit (BIOMOL International, Plymouth Meeting, PA). Triplicate samples containing 4  $\mu$ g of protein each were loaded in an opaque 96-well plate with Fluor de Lys substrate at a final concentration of 150  $\mu$ M. Following a 20 minute incubation at room temperature, 1  $\times$  Fluor de Lys developer with trichostatin A was added to stop the reaction and develop the fluorescent signal. Plates were read using a CytoFluor plate reader at 360 nm excitation and 440 nm emission wavelengths (Perkin Elmer, Waltham, MA). All samples were corrected to a buffer-only blank and normalized to the HeLa extract controls.

#### Western blot analysis

Western blot analysis on nuclear and cytoplasmic retinal protein fractions (see above) was performed as previously described [58] with the following modifications. Each fraction was loaded as a single lane (500  $\mu$ g) on separate 12% polyacrylamide gels and transblotted onto Immobilon P (Millipore, Inc, Billerica, MA). Membranes were stained with Ponceau S, cut into strips, and probed with various antibodies. Rabbit polyclonal antibodies for HDACs 1-5 (Santa Cruz, city CA) and anti-acetyl-histone H4 ChIP grade rabbit antiserum (Millipore, Inc) were used at a 1:100 dilution. Goat anti-rabbit secondary antibodies, conjugated to alkaline phosphatase, were used at a 1:500 dilution (Jackson ImmunoResearch Laboratories Inc, West Grove, PA). Blots were color developed using NBT and BCIP and digitally scanned.

#### Evaluation of transcripts in the retina by quantitative PCR

Total retinal RNA was isolated at 1, 3, and 7 days post ONC and 2  $\mu$ g was used for cDNA synthesis with reverse transcriptase and oligo(dT) [11]. The resulting cDNA was diluted 10-fold and 1  $\mu$ l was used for each qPCR reaction with SYBR Green PCR master mix (Applied Biosystems, Foster City, CA) and the appropriate HDAC primers (Table 1), as described previously [59]. Each primer set was optimized, and the resulting amplicon cloned and sequenced to confirm identity. Quantitative PCR was conducted on triplicate samples in each run using an ABI 7300 Real Time PCR system (Applied Biosystems). Transcript quantification was based on standard curves of each target amplicon and the absolute value for copy number was normalized to *S16* ribosomal protein mRNA. The values are expressed as the ratio of crush: control and normalized to the day 0 ratio that was set at 1.

In addition to evaluating individual transcripts in separate experiments, a qPCR mini array was developed that allowed us to examine 15 different mRNAs simultaneously during a single run. Each 96-well plate of the array contained triplicate assays for 5 RGC-specific genes (*Thy1*, *Brn3b*, *Scng*, *Nrn1*, *Fem1c*), 4 genes that are abundantly expressed in RGCs, and reportedly decline in expression, but are not necessarily RGC-specific (*TrkB*, *Nfl*, *Bclx*, *Tubb3*), 4 genes whose expression likely increase in damaged retinas (*Bim*, *Gap43*, *Hsp27*, *Gfap*), and 2 control genes (*Gad67* and *S16*). Two complete samples could be simultaneously examined on each plate. Primer design (Table 2) and PCR conditions were first normalized so that efficient amplification was obtained for all targets under the same PCR conditions. Sample quantification was carried out as described above, using a common standard curve for the entire plate.

#### Immunofluorescence and quantification of ACh4

Indirect immunofluorescence on 5  $\mu$ m thick retinal cryosections was done as described previously [60]. Primary antibodies included  $\gamma$ H2AX (monoclonal, Millipore, Inc), HDAC2, HDAC3, and ACh4 (previously mentioned) and were used at a 1:100 dilution. Secondary antibodies used were goat anti-rabbit with a Texas Red label (1:100) and goat anti-mouse with a FITC label (1:100) (both from Jackson ImmunoResearch Laboratories). The images were obtained using a Zeiss Axioplan 2 Imaging microscope with Axiovision 4.6.3.0 software (Carl Zeiss MicroImaging, Inc., Thornwood, NY) and viewed in Adobe Photoshop.

To quantify ACh4 staining, nuclear pixel intensity was measured in the ganglion cell (GCL) and inner nuclear layers (INL) using the outline function of the Zeiss Axiovision software. A minimum of 99 cells was counted in each layer and the mean pixel intensity per nucleus was calculated as a function of the nuclear area (in  $\mu$ m<sup>2</sup>). The calculated pixel intensity of GCL nuclei was normalized

**Table 1: Primers for ChIP and qPCR analysis**

| Gene Name    | Primer Sequences  | Size of product (bp) | Position <sup>a</sup> |
|--------------|---|----------------------|-----------------------|
| <i>Hdac1</i> | 5'-GTCAAAGGAGCCCACGCCAG-3'<br>5'-GTTGACAGCTTCGGGGAGGC-3'  | 603                  | +555/+1157            |
| <i>Hdac2</i> | 5'-ATGGCGTACAGTCAAGGAGG-3'<br>5'-AGCAACTGAACCACCCGTGG-3'  | 359                  | +209/+568             |
| <i>Hdac3</i> | 5'-GTATGACAGGACTGACGAGG-3'<br>5'-TTTCCTTCCCACCACAGAGG-3'  | 168                  | +528/+695             |
| <i>Hdac4</i> | 5'-CATCCCCAAGCCAAGCGAGC-3'<br>5'-CCGTCTGTAGCTCCTCCAGG-3'  | 619                  | +1521/+2140           |
| <i>Hdac5</i> | 5'-CTGTGCCTCATCAGGCCCTG-3'<br>5'-CCACGCTCAGCTTCTGCTGC-3'  | 642                  | +1919/+2560           |
| <i>Thy1</i>  | 5'-CTGGAATCAAAGGTGTGAGC-3'<br>5'-CCCCTCTTTATCCCCTTC-3'    | 190                  | -288/-98              |
| <i>Brn3b</i> | 5'-CTGAGGTCTGAAGCCAGAGC-3'<br>5'-ACGCCTGCTTGTTCAGG-3'     | 266                  | +17/+282              |
| <i>Fem1c</i> | 5'-TCCGCAGCCTTTCAGGATGC-3'<br>5'-AGTGCGCCTGCGTACTAAGG-3'  | 188                  | -255/-67              |
| <i>Nrn1</i>  | 5'-AACAAATCGAGTGGGCGCACC-3'<br>5'-AAGTACAGCCTCACGCCACG-3' | 251                  | -137/+114             |
| <i>BclX</i>  | 5'-ATCTGGTTCGATGGAGGAACC-3'<br>5'-AATCTATCTCCGGCGACAGC-3' | 214                  | +93/+326              |
| <i>Bim</i>   | 5'-AAAGCAAGGGCGGAGGGACG-3'<br>5'-CTGTCCTGCAGTTTGCGTGC-3'  | 238                  | -369/-132             |
| <i>cJun</i>  | 5'-AACACAAGCCGAAGCTGAGC-3'<br>5'-AGTCCTTATCCAGCCTGAGC-3'  | 263                  | -265/-2               |

<sup>a</sup> Indicates position (in base pairs) relative to the transcriptional start site (+1)

to the calculated pixel intensity of nuclei of the INL and the final calculated intensity was expressed as a ratio of crush:control.

#### Chromatin immunoprecipitation (ChIP) assays

Acetyl-histone H4 ChIP assays were performed as outlined by the manufacturer (Millipore). In each assay, 6 retinas were pooled and half of each sample was mixed with either AcH4 antibody or normal rabbit serum for a control (Jackson ImmunoResearch Laboratories). The supernatant obtained from the normal serum samples following immunoprecipitation was regarded as the input. DNA from immunoprecipitates was unlinked from protein complexes and purified further by phenol/chloroform extraction. Samples were analyzed in triplicate using qPCR as described above. The data obtained from qPCR were analyzed by subtracting the normal serum samples from the AcH4 immunoprecipitated samples and converting this to a percentage of the total input. These numbers were then expressed as a ratio of crush:control and normalized to the day 0 values.

#### HDAC inhibitor studies

To inhibit HDAC activity in the retina, TSA was injected either intraperitoneally (1 mg/kg in DMSO) 24 hours prior to ONC surgery or intravitreally (1 µl of 20 µM TSA in DMSO) immediately after ONC surgery. Vehicle injections consisted of an equal volume of DMSO. The effects of TSA on gene expression were conducted on *Fem1c*<sup>R3/+</sup> mice, which express the βGEO enzyme predominantly in RGCs in the retina. The level of βGeo expression was analyzed using two methods. Firstly, the level of βGEO activity in individual retinas was quantified by β-Galactosidase solution assay (Promega, Madison, WI) 5 days post ONC. The plates were read with an EL<sub>X</sub>800 microplate reader (Bio-Tek Instruments Inc., Winooski, VT). Duplicate samples of each eye was measured and total activity was calculated after subtraction of the β-Galactosidase activity measured in wild-type mice and corrected to the amount of total protein loaded in each sample. Secondly, βGEO expressing cells were identified histochemically, 5 days post ONC, by staining retinal preparations with X-Gal, followed by whole mounting as previously described



**Table 2: Primers for qPCR mini array analysis**

| Gene Name    | Primer Sequences  | Size of product (bp) |
|--------------|---|----------------------|
| <i>Thy1</i>  | 5'-CTTGCAGGTGTCCCGAGGGC-3'<br>5'-CTGAACCAGCAGGCTTATGC-3'  | 379                  |
| <i>Brn3b</i> | 5'-TCTTCCAACCCACCGAGC-3'<br>5'-GTGGTAAGTGGCGTCCGGCTTG-3'  | 157                  |
| <i>Sncg</i>  | 5'-GACCAAGCAGGGAGTAACGG-3'<br>5'-TCCAAGTCTCCTTGCGCAC-3'   | 240                  |
| <i>Nrn1</i>  | 5'-TTCCTGATCCTCGCGGTGC-3'<br>5'-TACTTTCGCCCTTCCTGGC-3'    | 238                  |
| <i>Fem1c</i> | 5'-GAAGTGTCCAACCCCATGG-3'<br>5'-TTGTCTGGGCATGGTGCG-3'     | 292                  |
| <i>TrkB</i>  | 5'-GTCTGACCTGATCCTGACGG-3'<br>X5'-CCCAACGTCCCAGTACAAGG-3' | 280                  |
| <i>Nfl</i>   | 5'-AGCACGAAGAGCGAGATGGC-3'<br>5'-TGCGAGCTCTGAGAGTAGCC-3'  | 173                  |
| <i>BclX</i>  | 5'-TTGACAATGGACTGGTTGA-3'<br>5'-GTAGAGTGGATGGTCAGTG-3'    | 780                  |
| <i>Tubb3</i> | 5'-GTTCTGGGAGGCATCAGCG-3'<br>5'-TCGGGCCTGAATAGGTGTCC-3'   | 207                  |
| <i>Bim</i>   | 5'-TCTGAGTGTGACAGAGAAGG-3'<br>5'-CTCCTGAGACTGTCGTATGG-3'  | 378                  |
| <i>Gap43</i> | 5'-TGAGCAAGCGAGCAGAAA-3'<br>5'-GCAGCCTTATGAGCCTTA-3'      | 199                  |
| <i>Hsp27</i> | 5'-CGCAACAGCAGTCATGTCGG-3'<br>5'-GGCTCACATCCAGAAACGCC-3'  | 257                  |
| <i>Gfap</i>  | 5'-CAAAGTGGCTGATGTCTACC-3'<br>5'-AGAACTGGATCTCCTCTCC-3'   | 269                  |
| <i>Gad67</i> | 5'-TCTTCCACTCCTTCGCTGC-3'<br>5'-GGAGAAGTCGGTCTCTGTGC-3'   | 279                  |
| <i>S16</i>   | 5'-CACTGCAAACGGGGAAATGG-3'<br>5'-TGAGATGGACTGTCGGATGG-3'  | 198                  |

All primer pairs were designed to span at least one intron.

[12]. To assess the effects of TSA on RGC loss, a 1 mg/kg intraperitoneal injection of TSA was administered 24 hours prior to ONC of adult CB6F1 mice. Two weeks after ONC, cells in the GCL were Nissl-stained and counted and compared to controls [33].

#### Statistical analysis

Data was collected from a minimum of 3 independent samples in all experiments, and shown as the mean  $\pm$  Standard Error in graphs. All statistical analyses were performed using the Student's *t*-test with statistical significance set at  $P \leq 0.05$ .

#### Additional material

**Additional file 1 Localization of HDACs 2 and 3 before and after optic nerve crush.** Photomicrographs of the individual channels for the merged images of Figure 3B. Sections from control retinas and retinas 3 days after optic nerve crush (ONC) were labeled with antibodies against HDAC2 or HDAC3 and counter-stained with DAPI to highlight nuclei. High-magnification images of the GCL are shown. (A, B) In control and crush retinas, HDAC2 labeling (red) was present in the nuclei of cells in the GCL, as determined by DAPI staining (blue). (C) In control retinas, HDAC3 labeling had a diffuse, cytoplasmic appearance with minimal overlap with nuclear DAPI staining. (D) At 3 days post ONC, many cells in the GCL exhibited nuclear HDAC3 labeling that coincided with DAPI staining of the nuclei. Scale bar = 5  $\mu$ m.

**Additional file 2 The deacetylation of histone H4 occurs in cells with nuclear  $\gamma$ H2AX and DNA fragmentation.** Sections from a retina after optic nerve injury were double labeled with antibodies against acetylated histone H4 (ACh4, green) and  $\gamma$ H2AX (red), to identify apoptotic cells, and counter-stained with DAPI (blue) to verify the nuclear presence of the proteins. Four cells in the ganglion cell layer are visible in various stages of cell death. DAPI-staining of 3 of the cells show condensed and fragmenting nuclei, consistent with apoptosis (arrows). One cell exhibits a normal nuclear staining pattern, including the presence of a robust nucleolus. Two of the cells with condensed chromatin also exhibit stage III  $\gamma$ H2AX staining and all 3 cells are weakly staining for ACh4. The relatively normal appearing cell exhibits both strong stage II  $\gamma$ H2AX (arrowhead) and ACh4 staining. A single representative nucleus, showing of DNA fragmentation and stage III  $\gamma$ H2AX labeling is indicated (N). Size bar = 5  $\mu$ m.

**Additional file 3 The change in expression and cellular distribution of  $\gamma$ H2AX provides a temporal indicator of histone deacetylation in damaged ganglion cells.** A graphic representation of the co-localization of  $\gamma$ H2AX staining and HDAC3 or Acetyl H4 (ACh4), indicates that HDAC3 is translocated into nuclei of apoptotic cells before the loss of ACh4 staining. The top row of cells represents the co-localization of  $\gamma$ H2AX with HDAC3, while the bottom row represents the co-localization of  $\gamma$ H2AX with ACh4. The labeling pattern of just  $\gamma$ H2AX is shown in the center row of cells. In each row,  $\gamma$ H2AX staining is depicted in red, while HDAC3 and ACh4 are depicted in green. At day 0, cells are negative for  $\gamma$ H2AX staining, with the exception of a spot adjacent to the nucleolus. These cells are classified as stage I, and exhibit cytosolic staining for HDAC3 and nuclear staining for ACh4. Once apoptosis is initiated,  $\gamma$ H2AX-staining appears as a perinuclear ring (stage II, principally detected at day 1 after optic nerve crush), which appears yellow in some cells co-stained for HDAC3 (Figures 6B and 12C), indicating complete co-localization. Some cells, however, appear to have a more orange ring with a green nucleus, suggesting movement of HDAC3 from the cytosol to the nucleus in stage II cells (Figures 6B asterisk, 6C, 12E). In cells with nuclear  $\gamma$ H2AX-staining (stage III, detected in increasing amounts at 3, 5, and 7 days post optic nerve crush), cells co-labeled for HDAC3 exhibit yellow to orange nuclei, indicating co-localization of these proteins (Figures 6D-F, 12H, 12J). With respect to ACh4 labeling, stage I cells exhibit bright green nuclei. Stage II cells typically appear as red rings of  $\gamma$ H2AX label surrounding green nuclei (Figures 7B, 12C). Stage III cells exhibit three different nuclear colors, indicative of the extent of ACh4 label present, and appear to progress from yellow (Figures 7D, 12F), to orange (Figures 7E, 12G), to red (Figures 7F, 12I). Orange to red nuclei are often misshapen, although DAPI staining confirms the presence of condensed and fragmented DNA in these structures (See additional file 2).

#### Authors' contributions

HRP participated in the design of this experiment, conducted the HDAC activity assays, immunofluorescence studies, ChIP assays, qPCR experiments, whole-mount staining, cell counts, analyzed the data, and drafted the manuscript. CLS performed the Western Blot analysis, assisted with the immunofluorescence experiments, analyzed the data, and contributed to the drafting of the manuscript. RWN conceived of this experiment, performed the optic nerve crush, and helped draft the manuscript. All authors read and approved the final manuscript.

#### Acknowledgements

This work was funded by grants from the National Eye Institute (R01 EY12223 to R.W.N. and CORE grant P30 EY016665), an unrestricted research grant from Research to Prevent Blindness, and the RPB Wasserman Award (to R.W.N.). The authors would also like to thank Dr. Shiming Chen for providing assistance with the HDAC inhibitor treatment protocol, Joel Dietz for his assistance in conducting qPCR experiments, Katherine Janssen and Dr. Sheila Semaan for assistance with the  $\beta$ -Galactosidase assays, and Drs. Donald Zack and Zhiyong Yang for providing quantitative data for ganglion cell specific gene expression from their microarray studies.

#### Author Details

<sup>1</sup>Department of Biomolecular Chemistry, University of Wisconsin, 1300 University Ave, 6671 MSC, Madison, WI, 53706, USA, <sup>2</sup>Department of Ophthalmology and Visual Science, University of Wisconsin, 3310 University Ave, Suite 206, Madison, WI, 53706, USA and <sup>3</sup>Department of Physiology, University of Wisconsin, 1300 University Ave, 125 SMI, Madison, WI 53706, USA

Received: 16 November 2009 Accepted: 26 May 2010

Published: 26 May 2010

#### References

1. Chang LK, Putcha GV, Deshmukh M, Johnson EM Jr: **Mitochondrial involvement in the point of no return in neuronal apoptosis.** *Biochimie* 2002, **84**(2-3):223-231.
2. Cha JH: **Transcriptional dysregulation in Huntington's disease.** *Trends Neurosci* 2000, **23**(9):387-392.
3. Ahmed F, Brown KM, Stephan DA, Morrison JC, Johnson EC, Tomarev SI: **Microarray analysis of changes in mRNA levels in the rat retina after experimental elevation of intraocular pressure.** *Invest Ophthalmol Vis Sci* 2004, **45**(4):1247-1258.
4. Soto I, Oglesby E, Buckingham BP, Son JL, Roberson ED, Steele MR, Inman DM, Vetter ML, Horner PJ, Marsh-Armstrong N: **Retinal ganglion cells downregulate gene expression and lose their axons within the optic nerve head in a mouse glaucoma model.** *J Neurosci* 2008, **28**(2):548-561.
5. Yang Z, Quigley HA, Pease ME, Yang Y, Qian J, Valenta D, Zack DJ: **Changes in gene expression in experimental glaucoma and optic nerve transection: the equilibrium between protective and detrimental mechanisms.** *Invest Ophthalmol Vis Sci* 2007, **48**(12):5539-5548.
6. Sugars KL, Rubinsztein DC: **Transcriptional abnormalities in Huntington disease.** *Trends Genet* 2003, **19**(5):233-238.
7. Duke DC, Moran LB, Pearce RK, Graeber MB: **The medial and lateral substantia nigra in Parkinson's disease: mRNA profiles associated with higher brain tissue vulnerability.** *Neurogenetics* 2007, **8**(2):83-94.
8. Ferraiuolo L, Heath PR, Holden H, Kasher P, Kirby J, Shaw PJ: **Microarray analysis of the cellular pathways involved in the adaptation to and progression of motor neuron injury in the SOD1 G93A mouse model of familial ALS.** *J Neurosci* 2007, **27**(34):9201-9219.
9. Chou AH, Yeh TH, Ouyang P, Chen YL, Chen SY, Wang HL: **Polyglutamine-expanded ataxin-3 causes cerebellar dysfunction of SCA3 transgenic mice by inducing transcriptional dysregulation.** *Neurobiol Dis* 2008, **31**(1):89-101.
10. Blalock EM, Geddes JW, Chen KC, Porter NM, Markesbery WR, Landfield PW: **Incipient Alzheimer's disease: microarray correlation analyses reveal major transcriptional and tumor suppressor responses.** *Proc Natl Acad Sci USA* 2004, **101**(7):2173-2178.
11. Schlamp CL, Johnson EC, Li Y, Morrison JC, Nickells RW: **Changes in Thy1 gene expression associated with damaged retinal ganglion cells.** *Mol Vis* 2001, **7**:192-201.
12. Schlamp CL, Thliveris AT, Li Y, Kohl LP, Knop C, Dietz JA, Larsen IV, Imesch P, Pinto LH, Nickells RW: **Insertion of the beta Geo promoter trap into the Fem1c gene of ROSA3 mice.** *Mol Cell Biol* 2004, **24**(9):3794-3803.
13. Chidlow G, Casson R, Sobrado-Calvo P, Vidal-Sanz M, Osborne NN: **Measurement of retinal injury in the rat after optic nerve transection: an RT-PCR study.** *Mol Vis* 2005, **11**:387-396.
14. Levin LA, Schlamp CL, Spielfeld RL, Geszvain KM, Nickells RW: **Identification of the bcl-2 family of genes in the rat retina.** *Invest Ophthalmol Vis Sci* 1997, **38**(12):2545-2553.
15. Weishaupt JH, Klocker N, Bahr M: **Axotomy-induced early down-regulation of POU-IV class transcription factors Brn-3a and Brn-3b in retinal ganglion cells.** *J Mol Neurosci* 2005, **26**(1):17-25.
16. Ivanov D, Dvorianchikova G, Nathanson L, McKinnon SJ, Shestopalov VI: **Microarray analysis of gene expression in adult retinal ganglion cells.** *FEBS Lett* 2006, **580**(1):331-335.
17. Cheng L, Sapieha P, Kittlerova P, Hauswirth WW, Di Polo A: **TrkB gene transfer protects retinal ganglion cells from axotomy-induced death in vivo.** *J Neurosci* 2002, **22**(10):3977-3986.

18. Napankangas U, Lindqvist N, Lindholm D, Hallbook F: **Rat retinal ganglion cells upregulate the pro-apoptotic BH3-only protein Bim after optic nerve transection.** *Brain Res Mol Brain Res* 2003, **120**(1):30-37.
19. Park KH, Cozier F, Ong OC, Caprioli J: **Induction of heat shock protein 72 protects retinal ganglion cells in a rat glaucoma model.** *Invest Ophthalmol Vis Sci* 2001, **42**(7):1522-1530.
20. McKinnon SJ, Lehman DM, Kerrigan-Baumrind LA, Merges CA, Pease ME, Kerrigan DF, Ransom NL, Tahzib NG, Reitsamer HA, Levkovich-Verbin H, Quigley HA, Zack DJ: **Caspase activation and amyloid precursor protein cleavage in rat ocular hypertension.** *Invest Ophthalmol Vis Sci* 2002, **43**(4):1077-1087.
21. Huang W, Fileta J, Guo Y, Grosskreutz CL: **Downregulation of Thy1 in retinal ganglion cells in experimental glaucoma.** *Curr Eye Res* 2006, **31**(3):265-271.
22. Jenuwein T, Allis CD: **Translating the histone code.** *Science* 2001, **293**(5532):1074-1080.
23. de la Cruz X, Lois S, Sanchez-Molina S, Martinez-Balbas MA: **Do protein motifs read the histone code?** *Bioessays* 2005, **27**(2):164-175.
24. Shahbazian MD, Grunstein M: **Functions of site-specific histone acetylation and deacetylation.** *Annu Rev Biochem* 2007, **76**:75-100.
25. Bottomley MJ: **Structures of protein domains that create or recognize histone modifications.** *EMBO Rep* 2004, **5**(5):464-469.
26. Lahm A, Paolini C, Pallaoro M, Nardi MC, Jones P, Neddermann P, Sambucini S, Bottomley MJ, Lo Surdo P, Carfi A, Koch U, De Francesco R, Steinkuhler C, Gallinari P: **Unraveling the hidden catalytic activity of vertebrate class IIa histone deacetylases.** *Proc Natl Acad Sci USA* 2007, **104**(44):17335-17340.
27. de Ruijter AJ, van Gennip AH, Caron HN, Kemp S, van Kuilenburg AB: **Histone deacetylases (HDACs): characterization of the classical HDAC family.** *Biochem J* 2003, **370**(Pt 3):737-749.
28. Longworth MS, Laimins LA: **Histone deacetylase 3 localizes to the plasma membrane and is a substrate of Src.** *Oncogene* 2006, **25**(32):4495-4500.
29. Sengupta N, Seto E: **Regulation of histone deacetylase activities.** *J Cell Biochem* 2004, **93**(1):57-67.
30. Li Y, Schlamp CL, Nickells RW: **Experimental induction of retinal ganglion cell death in adult mice.** *Invest Ophthalmol Vis Sci* 1999, **40**(5):1004-1008.
31. Andreau K, Castedo M, Perfettini JL, Roumier T, Pichart E, Souquere S, Vivet S, Larochette N, Kroemer G: **Preapoptotic chromatin condensation upstream of the mitochondrial checkpoint.** *J Biol Chem* 2004, **279**(53):55937-55945.
32. Drager UC, Olsen JF: **Ganglion cell distribution in the retina of the mouse.** *Invest Ophthalmol Vis Sci* 1981, **20**(3):285-293.
33. Li Y, Semaan SJ, Schlamp CL, Nickells RW: **Dominant inheritance of retinal ganglion cell resistance to optic nerve crush in mice.** *BMC Neurosci* 2007, **8**:19.
34. Quigley HA, Nickells RW, Kerrigan LA, Pease ME, Thibault DJ, Zack DJ: **Retinal ganglion cell death in experimental glaucoma and after axotomy occurs by apoptosis.** *Invest Ophthalmol Vis Sci* 1995, **36**(5):774-786.
35. Libby RT, Li Y, Savinova OV, Barter J, Smith RS, Nickells RW, John SW: **Susceptibility to neurodegeneration in a glaucoma is modified by Bax gene dosage.** *PLoS Genet* 2005, **1**(1):17-26.
36. Li Y, Kao GD, Garcia BA, Shabanowitz J, Hunt DF, Qin J, Phelan C, Lazar MA: **A novel histone deacetylase pathway regulates mitosis by modulating Aurora B kinase activity.** *Genes Dev* 2006, **20**(18):2566-2579.
37. Rouaux C, Jokic N, Mbebi C, Boutillier S, Loeffler JP, Boutillier AL: **Critical loss of CBP/p300 histone acetylase activity by caspase-6 during neurodegeneration.** *Embo J* 2003, **22**(24):6537-6549.
38. Steffan JS, Bodai L, Pallos J, Poelman M, McCampbell A, Apostol BL, Kazantsev A, Schmidt E, Zhu YZ, Greenwald M, Kurokawa R, Housman DE, Jackson GR, Marsh JL, Thompson LM: **Histone deacetylase inhibitors arrest polyglutamine-dependent neurodegeneration in Drosophila.** *Nature* 2001, **413**(6857):739-743.
39. Klose RJ, Zhang Y: **Regulation of histone methylation by demethylimination and demethylation.** *Nat Rev Mol Cell Biol* 2007, **8**(4):307-318.
40. Klose RJ, Yan Q, Tothova Z, Yamane K, Erdjument-Bromage H, Tempst P, Gilliland DG, Zhang Y, Kaelin WG Jr: **The retinoblastoma binding protein RBP2 is an H3K4 demethylase.** *Cell* 2007, **128**(5):889-900.
41. Karagianni P, Wong J: **HDAC3: taking the SMRT-N-CoRrect road to repression.** *Oncogene* 2007, **26**(37):5439-5449.
42. Boutillier AL, Trinh E, Loeffler JP: **Selective E2F-dependent gene transcription is controlled by histone deacetylase activity during neuronal apoptosis.** *J Neurochem* 2003, **84**(4):814-828.
43. Karagiannis TC, El-Osta A: **Clinical potential of histone deacetylase inhibitors as stand alone therapeutics and in combination with other chemotherapeutics or radiotherapy for cancer.** *Epigenetics* 2006, **1**(3):121-126.
44. Jiang H, Nucifora FC Jr, Ross CA, DeFranco DB: **Cell death triggered by polyglutamine-expanded huntingtin in a neuronal cell line is associated with degradation of CREB-binding protein.** *Hum Mol Genet* 2003, **12**(1):1-12.
45. Jin K, Mao XO, Simon RP, Greenberg DA: **Cyclic AMP response element binding protein (CREB) and CREB binding protein (CBP) in global cerebral ischemia.** *J Mol Neurosci* 2001, **16**(1):49-56.
46. McCampbell A, Taye AA, Whitty L, Penney E, Steffan JS, Fischbeck KH: **Histone deacetylase inhibitors reduce polyglutamine toxicity.** *Proc Natl Acad Sci USA* 2004, **98**(26):15179-15184.
47. Pallos J, Bodai L, Lukacsovich T, Purcell JM, Steffan JS, Thompson LM, Marsh JL: **Inhibition of specific HDACs and sirtuins suppresses pathogenesis in a Drosophila model of Huntington's disease.** *Hum Mol Genet* 2008, **17**(23):3767-3775.
48. Hockly E, Richon VM, Woodman B, Smith DL, Zhou X, Rosa E, Sathasivam K, Ghazi-Noori S, Mahal A, Lowden PA, Steffan JS, Marsh JL, Thompson LM, Lewis CM, Marks PA, Bates GP: **Suberoylanilide hydroxamic acid, a histone deacetylase inhibitor, ameliorates motor deficits in a mouse model of Huntington's disease.** *Proc Natl Acad Sci USA* 2003, **100**(4):2041-2046.
49. Saha RN, Pahan K: **HATs and HDACs in neurodegeneration: a tale of discordant acetylation homeostasis.** *Cell Death Differ* 2006, **13**(4):539-550.
50. Ryu H, Lee J, Olofsson BA, Mwidau A, Dedeoglu A, Escudero M, Flemington E, Azizkhan-Clifford J, Ferrante RJ, Ratan RR: **Histone deacetylase inhibitors prevent oxidative neuronal death independent of expanded polyglutamine repeats via an Sp1-dependent pathway.** *Proc Natl Acad Sci USA* 2003, **100**(7):4281-4286.
51. Chen B, Cepko CL: **HDAC4 regulates neuronal survival in normal and diseased retina.** *Science* 2009, **323**(5911):256-259.
52. Seo HW, Kim EJ, Na H, Lee MO: **Transcriptional activation of hypoxia-inducible factor-1alpha by HDAC4 and HDAC5 involves differential recruitment of p300 and FIH-1.** *FEBS Lett* 2009, **583**(1):55-60.
53. Weber AJ, Harman CD: **BDNF preserves the dendritic morphology of alpha and beta ganglion cells in the cat retina after optic nerve injury.** *Invest Ophthalmol Vis Sci* 2008, **49**(6):2456-2463.
54. Li Y, Schlamp CL, Poulsen KP, Nickells RW: **Bax-dependent and independent pathways of retinal ganglion cell death induced by different damaging stimuli.** *Exp Eye Res* 2000, **71**(2):209-213.
55. Bortner CD, Sifre MI, Cidlowski JA: **Cationic gradient reversal and cytoskeleton-independent volume regulatory pathways define an early stage of apoptosis.** *J Biol Chem* 2008, **283**:7219-7229.
56. Redman PT, He K, Hartnett KA, Jefferson BS, Hu L, Rosenberg PA, Levitan ES, Aizenman E: **Apoptotic surge of potassium currents is mediated by p38 phosphorylation of Kv2.1.** *Proc Natl Acad Sci USA* 2007, **104**(3568):3573.
57. Koeberle PD, Wang Y, Schlichter LC: **Kv1.1 and Kv1.3 channels contribute to the degeneration of retinal ganglion cells after optic nerve transection in vivo.** *Cell Death Differ* 2010, **17**:134-44.
58. Azarian SM, Schlamp CL, Williams DS: **Characterization of calpain II in the retina and photoreceptor outer segments.** *J Cell Sci* 1993, **105**(Pt 3):787-798.
59. Pelzel HR, Schlamp CL, Poulsen GL, Ver Hoeve JA, Nork TM, Nickells RW: **Decrease of cone opsin mRNA in experimental ocular hypertension.** *Mol Vis* 2006, **12**(1272):1282.
60. Schlamp CL, Nickells RW: **Light and dark cause a shift in the spatial expression of a neuropeptide-processing enzyme in the rat retina.** *J Neurosci* 1996, **16**(7):2164-2171.

61. Blanchard F, Chipoy C: **Histone deacetylase inhibitors: new drugs for the treatment of inflammatory diseases?** *Drug Discov Today* 2005, **10**(3):197-204.
62. Khan N, Jeffers M, Kumar S, Hackett C, Boldog F, Khramtsov N, Qian X, Mills E, Berghs SC, Carey N, Finn PW, Collins LS, Tumber A, Ritchie JW, Jensen PB, Lichenstein HS, Sehested M: **Determination of the class and isoform selectivity of small-molecule histone deacetylase inhibitors.** *Biochem J* 2008, **409**(2):581-589.

doi: 10.1186/1471-2202-11-62

**Cite this article as:** Pelzel *et al.*, Histone H4 deacetylation plays a critical role in early gene silencing during neuronal apoptosis *BMC Neuroscience* 2010, **11**:62

**Submit your next manuscript to BioMed Central  
and take full advantage of:**

- Convenient online submission
- Thorough peer review
- No space constraints or color figure charges
- Immediate publication on acceptance
- Inclusion in PubMed, CAS, Scopus and Google Scholar
- Research which is freely available for redistribution

Submit your manuscript at  
[www.biomedcentral.com/submit](http://www.biomedcentral.com/submit)

